AD-A079 943 IRT CORP SAN DIEGO CA F/G 20/14

DYNACYL PREDICTIONS OF AIR PRESSURE EFFECTS ON ELECTRON-BEAM IE--ETC(U)

DEC 78 T BUCKMAN DNA001-77-C-0285

UNCLASSIFIED IRT-8168-003 DNA-4793F NL

END
DATE
FILMED
2 80
DDC

AD-E 300 647

12 LEVEL III

DNA 4793F

DYNACYL PREDICTIONS OF AIR PRESSURE EFFECTS ON ELECTRON-BEAM IEMP

IRT Corporation
P.O. Box 80817
San Diego, California 92138

28 December 1978

Final Report for Period 10 October 1977—31 October 1978

CONTRACT No. DNA 001-77-C-0285

APPROVED FOR PUBLIC RELEASE;
DISTRIBUTION UNLIMITED.

THIS WORK SPONSORED BY THE DEFENSE NUCLEAR AGENCY
UNDER RDT&E RMSS CODE B323077464 R99QAXEE50112 H2590D.

Prepared for
Director
DEFENSE NUCLEAR AGENCY
Washington, D. C. 20305

Destroy this report when it is no longer needed. Do not return to sender.

PLEASE NOTIFY THE DEFENSE NUCLEAR AGENCY, ATTN: STTI, WASHINGTON, D.C. 20305, IF YOUR ADDRESS IS INCORRECT, IF YOU WISH TO BE DELETED FROM THE DISTRIBUTION LIST, OR IF THE ADDRESSEE IS NO LONGER EMPLOYED BY YOUR ORGANIZATION.

UNCLASSIFIED

SECURITY CLASSIFICATION OF THIS PAGE (When Data Entered)

REPORT DOCUMENTATION PAGE

READ INSTRUCTIONS BEFORE COMPLETING FORM

1. REPORT NUMBER: DNA 4793F
2. GOVT ACCESSION NO.:
3. RECIPIENT'S CATALOG NUMBER:

4. ~~TITLE (and Subtitle)~~: DYNACYL PREDICTIONS OF AIR PRESSURE EFFECTS ON ELECTRON-BEAM IEMP

5. TYPE OF REPORT & PERIOD COVERED: Final Report for Period 31 Oct 77—31 Oct 78

6. PERFORMING ORG. REPORT NUMBER: IRT-8168-003

7. AUTHOR(s): T. Buckman

8. CONTRACT OR GRANT NUMBER(s): DNA 001-77-C-0285

9. PERFORMING ORGANIZATION NAME AND ADDRESS:
IRT Corporation
P.O. Box 80817
San Diego, California 92138

10. PROGRAM ELEMENT, PROJECT, TASK AREA & WORK UNIT NUMBERS: Subtask R99QAXEE501-12

11. CONTROLLING OFFICE NAME AND ADDRESS:
Director
Defense Nuclear Agency
Washington, D.C. 20305

12. ~~REPORT DATE~~: 28 December 1978

13. NUMBER OF PAGES: 54

14. MONITORING AGENCY NAME & ADDRESS (if different from Controlling Office): Final rpt. 31 Oct 77 - 31 Oct 78

15. SECURITY CLASS (of this report): UNCLASSIFIED

15a. DECLASSIFICATION/DOWNGRADING SCHEDULE

16. DISTRIBUTION STATEMENT (of this Report)

Approved for public release; distribution unlimited.

17. DISTRIBUTION STATEMENT (of the abstract entered in Block 20, if different from Report)

DNA, SPIE

18. SUPPLEMENTARY NOTES

This work sponsored by the Defense Nuclear Agency under RDT&E RMSS Code B323077464 R99QAXEE50112 H2590D.

19. KEY WORDS (Continue on reverse side if necessary and identify by block number)

Internal Electromagnetic Pulse
Air Pressure Effects
DYNACYL
Numerical Simulation

20. ABSTRACT (Continue on reverse side if necessary and identify by block number)

The DYNACYL computer code has been used to predict the effect of air pressure on the currents and fields inside a right-circular cylinder irradiated on one end with a pulse-electron beam. Description of the incident beam was provided by the Harry Diamond Laboratories and was used to determine the value for the input variables. The results presented in this document will be used by Harry Diamond Laboratories for the Defense Nuclear Agency.

DD FORM 1 JAN 73 1473 EDITION OF 1 NOV 65 IS OBSOLETE

UNCLASSIFIED

SECURITY CLASSIFICATION OF THIS PAGE (When Data Entered)

TABLE OF CONTENTS

1. INTRODUCTION 5
2. DESCRIPTION OF THE PROBLEM 6
3. DESCRIPTION OF CODE 8
4. DESCRIPTION OF CODE INPUT 9
5. LISTING OF CODE INPUT 10
6. DISCUSSION OF RESULTS 15
7. RECOMMENDATIONS 17

REFERENCES 49

LIST OF FIGURES

Figure		
1	Average measured beam current and measured beam energy as functions of time	7
2	Details of the cylinder geometry	7
3	Radial current $I_r(t)$ on the end plate at z = 55 cm for different values of r at a pressure of 2 mtorr	28
4	Radial current $I_r(t)$ on the end plate at z = 55 cm for different values of r at a pressure of 100 mtorr	29
5	Radial current $I_r(t)$ on the end plate at z = 55 cm for different values of r at a pressure of 300 mtorr	30
6	Radial current $I_r(t)$ on the end plate at z = 55 cm for different values of r at a pressure of 50 torr	31
7	Total space current $I_t(t)$ at five different values of z at a pressure of 2 mtorr	32
8	Total space current $I_t(t)$ at five different values of z at a pressure of 100 mtorr	33
9	Total space current $I_t(t)$ at five different values of z at a pressure of 300 mtorr	34
10	Total space current $I_t(t)$ at five different values of z at a pressure of 50 torr	35
11	$H\phi(t)$ evaluated at r = 13.8 cm for five different values of z at a pressure of 2 mtorr	36
12	$H\phi(t)$ evaluated at r = 13.8 cm for five different values of z at a pressure of 100 mtorr	37
13	$H\phi(t)$ evaluated at r = 13.8 cm for five different values of z at a pressure of 300 mtorr	38
14	$H\phi(t)$ evaluated at r = 13.8 cm for five different values of z at a pressure of 50 torr	39
15	$E_r(t)$ at z = 2.5, 50 cm; r = 14.6 cm and a pressure of 2 mtorr	40
16	$E_r(t)$ at z = 2.5, 50 cm; r = 14.6 cm and a pressure of 100 mtorr	41
17	$E_r(t)$ at z = 3.5, 50 cm; r = 14.6 cm and a pressure of 300 mtorr	42
18	$E_r(t)$ at z = 2.5, 50 cm; r = 14.6 cm and a pressure of 50 torr	43
19	$E_z(t)$ at z = 0, 32.5, and 55 cm; r = 0 and a pressure of 2 mtorr	44
20	$E_z(t)$ at z = 0, 32.5, and 55 cm; r = 0 and a pressure of 100 mtorr	45
21	$E_z(t)$ at z = 0, 32.5, and 55 cm; r = 0 and a pressure of 300 mtorr	46
22	$E_z(t)$ at z = 0, 32.5, and 55 cm; r = 0 and a pressure of 50 torr	47

LIST OF TABLES

Table		
1	Current Time Point Pairs Used to Describe Input Pulse Shape	11
2	Beam Energy Time History and Emission Energy Spectra	12
3	Emission Angular Spectra	14
4	Additional DYNACYL Input Variables	14
5	Computed Values of $H\phi(t)$ at Constant r, Different Values of z	18
6	Computed Values of $H\phi(t)$ at Constant r, Different Values of r	19
7	Computed Values of $H\phi(t)$ at Constant r, Different Values of z	20
8	Computed Values of $H\phi(t)$ at Constant r, Different Values of z	21
9	Total Space Current at Different Values of z	22
10	Total Space Current at Different Values of z	23
11	Total Space Current at Different Values of z	24
12	Total Space Current at Different Values of z	25
13	Computed Values of End Plate Current, Axial and Radial E Fields at a pressure of 2 mtorr	26
14	Computed Values of End Plate Current, Axial and Radial E Fields at a pressure of 300 mtorr	27

1. INTRODUCTION

The information presented in this document is a continuation of the work described in Reference 2. This document presents the predictions made by IRT for IEMP problem 4 whereas the earlier report presented results for problems 2 and 3. Both reports are part of the internal SGEMP IEMP code validation program being conducted by Harry Diamond laboratories for the Defense Nuclear Agency.

The primary purpose of the code validation program is to test the ability of existing SGEMP codes to successfully account for air pressure effects on the internal system generated electromagnetic pulse. The presence of even small amounts of air inside a system cavity can cause significant variations in IEMP waveforms. The conclusions drawn from earlier work in this area (Ref 1) focus on the inability of existing codes to treat air ionization effects at pressures in the hundreds of mtorr range, the regime of avalanche ionization for the pulse parameters described in this report.

The predictions were made using the DYNACYL computer code (Ref 2). DYNACYL is a *fully dynamic, finite difference, time domain* approach to solving Maxwell's equations incorporates self-consistent particle tracking. IEMP problem 4 is similar in geometry to problems 2 and 3. However, an attempt has been made to more accurately characterize the incident electron pulse characteristics.

2. DESCRIPTION OF THE PROBLEM

IEMP problem 4 considers the injection of a pulsed electron beam through a Mylar plus wire mesh membrane into one end of a circular cylinder. The average measured beam current and measured beam energy are shown as functions of time in Figure 1. The pulse has a total duration of 22.5 ns with an approximate zero-to-peak rise time of 6.4 ns. Maximum average energy of the beam is 200 KeV. The cylinder used in the problem was constructed from a conducting material, with a length of 55 cm, and a radius of 15.4 cm as shown in Figure 2. One end of the cylinder was left open. The Mylar wire mesh screen with attached cylinder was used to construct an enclosed chamber where only small quantities of air were allowed to remain. The air pressure inside the chamber was the controlled variable in the experiment and was fixed at four values, either 0.002, 0.1, 0.3 or 50 torr.

The computational requirements for the problem were to determine values of current, and values for the electric and magnetic field intensity as a function of time and pressure at several locations inside the cylinder.

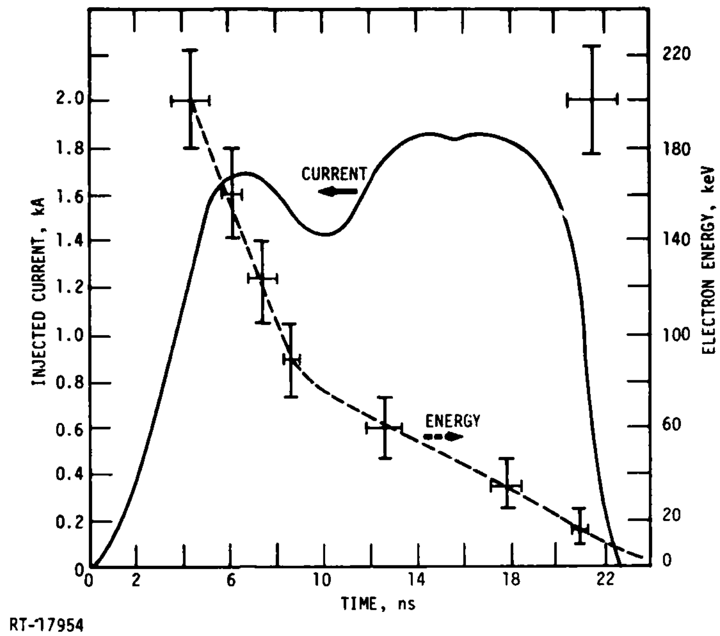

Figure 1. Average measured beam current and measured beam energy as functions of time

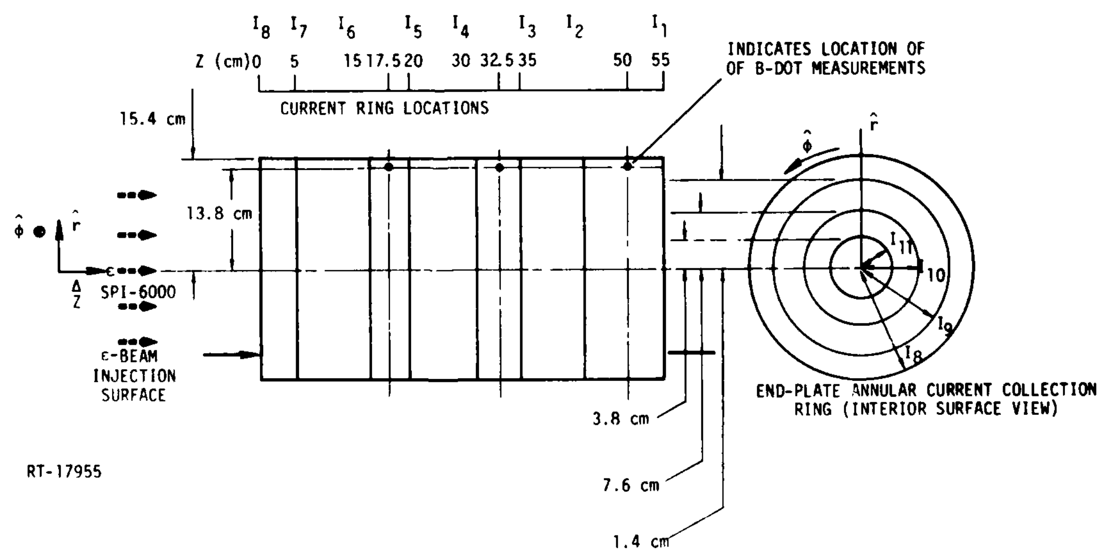

Figure 2. Details of the cylinder geometry

3. DESCRIPTION OF CODE

DYNACYL solves two dimensional, time dependent IEMP problems for a circular cylinder when one end emits electrons to the interior in an axisymmetric distribution. The electrons are modeled by quasi-particles, where each particle may represent a large number of electrons. The particles are injected into the spatial grid at various energies, angles, and charges depending on the description of the incident pulse inputed to the program. The particles of charge have their motions computed via Newtonian equations of motion and are responsible for ionization of air molecules present in the cylinder. The motion of these secondary electrons is described by an empirical drift velocity and the rate of ionization by these secondary electrons is also described empirically. The total charge motion information is converted into a current density expression via the continuity equation which in turn is used as a source term in generating the solution to Maxwell's equations.

4. DESCRIPTION OF CODE INPUT

DYNACYL requires a description of the pulse shape both as a function of time and space and a description of the average energy of the pulse as a function of time and space. The pulse shape is described in time by defining up to 41 magnitude time point pairs to the program. The spatial description of the pulse is limited to specifying variations in the pulse magnitude as a function of radial position. This single degree of freedom is further limited by requiring the user of DYNACYL to choose either no variation with respect to radius or a Gaussian variation with respect to radius. However, the code can and has been modified to accept other descriptions.

Up to 10 different energy spectrums can be specified with respect to the time variation of the average energy. These spectra are defined at different points in time and the code linearly interpolates between spectra to obtain spectral information at other points in time. The spectral information is inputed to the code with numbers which essentially represent a histogram type format. Two histograms are used to define the spectrum at any one instant of time. One of the histograms gives information on particle energy levels. The other histogram gives information on emission angles of the particles.

All of the aforementioned information is used to define a time varying vector field over the emission face of the cylinder. This field describes the velocity, point of entry, angle of entry, and charge associated with paticles entering the cylinder. The number of entry points are defined by the user and are linearly spaced with respect to the radius. The maximum number of entry points that can be defined at this time, are 20.

5. LISTING OF CODE INPUT

The following tables list the actual values of various input variables read into DYNACYL. One should notice that a stronger emphasis has been placed on describing the pulse and its associated spectra than was done in problems two and three. However, not as many spatial zones and particle emission points have been defined in problem four as was done in the previous two problems. These choices should be viewed as a shift in emphasis while attempting to maintain computational efficiency.

Table 1 lists 28 magnitude-time point pairs, which were used to delineate the shape of the incident pulse. Table 2 lists ten different energy spectra, each one with seven energy bins, that were used to describe the energy time history of the pulse. Table 3 lists the single emission angle spectrum which is used to describe the distribution with respect to angle of the emitted particles for all time t. The use of only one emission angle spectrum is a requirement of DYNACYL.

Finally, Table 4 lists several additional variables required by DYNACYL along with the values which were inputed to the code. The reasons behind selecting the particular values shown are, in some cases, quite complex. It sufficies to say, at this point, that operational constraints of DYNACYL along with a desire to maintain computational efficiency precipated many of the choices.

Table 1. Current Time Points Pairs Used to Describe Input Pulse Shape

Time (nsec)	Pulse Amplitude (K amps)
0	0
1.1	.15
2.0	.37
5.3	1.56
5.7	1.65
6.4	1.70
7.1	1.70
7.7	1.65
8.4	1.58
9.2	1.46
9.6	1.43
10.4	1.43
11.1	1.47
12.6	1.76
13.4	1.82
14.4	1.84
15.1	1.84
15.7	1.83
16.4	1.84
17.2	1.84
18.0	1.82
19.1	1.74
20.0	1.63
20.5	1.44
21.5	.58
21.7	.38
22.0	.20
22.8	0

Table 2. Beam Energy Time History and Emission Energy Spectra

Time (nsec)	Average Beam Energy (KeV)	Spectra Energy Bin Edges (KeV)	Relative Intensity
0	190	196.0	0.095
		195.0	0.225
		194.0	0.245
		193.0	0.155
		192.0	0.115
		191.0	0.100
		189.0	0.065
		186.0	
4.2	190	Same as above	Same as above
5.2	180	175.0	0.065
		174.0	0.200
		173.0	0.205
		172.0	0.170
		171.0	0.140
		170.0	0.150
		169.0	0.070
		165.0	
6.2	150	145.0	0.065
		144.5	0.158
		143.5	0.180
		142.5	0.163
		141.5	0.140
		140.5	0.241
		136.5	0.053
		131.5	
7.4	120	114.0	0.01
		113.0	0.115
		112.0	0.200
		111.0	0.165
		110.0	0.125
		109.0	0.255
		104.0	0.133
		95.0	
8.2	100	92.0	0.210
		90.0	0.290
		88.0	0.195
		86.0	0.090
		84.0	0.065
		82.0	0.075
		76.0	0.075
		68.0	

Table 2. Beam Energy Time History and Emission Energy Spectra (Continued)

Time (nsec)	Average Beam Energy (KeV)	Spectra Energy Bin Edges (KeV)	Relative Intensity
8.6	90	85.0	0.080
		80.0	0.540
		75.0	0.190
		70.0	0.070
		65.0	0.040
		60.0	0.020
		55.0	0.010
		50.0	
9.6	80	72.0	0.160
		68.0	0.380
		64.0	0.180
		60.0	0.100
		56.0	0.050
		52.0	0.060
		44.0	0.070
		36.0	
11.2	70	60.0	0.070
		57.0	0.250
		54.0	0.200
		51.0	0.150
		48.0	0.095
		39.0	0.125
		30.0	
15.2	50	36.0	0.100
		30.0	0.104
		28.0	0.114
		26.0	0.302
		20.0	0.242
		14.0	0.092
		6.0	0.146
		2.0	

Table 3. Emission Angular Spectra

Spectra Angle Bin Edges (degrees)	Relative Intensity
0	0.0200
5	0.0450
10	0.1475
20	0.1650
30	0.1975
40	0.1675
50	0.1050
60	0.0975
70	0.0550
80	

Table 4. Additional DYNACYL Input Variables

Additional Emission Variables	
Peak value of current density on axis	3.12 amp/cm^2
Peak value of current density at cylinder wall	2.08 amp/cm^2
No. of radial positions from which particle are emitted	4
Spatial Zoning Variables	
No. of radial zones	4
No. of azimuthal zones	4
No. of axial zones	11
Time Variables	
Maximum time	36 nsec
Time steps	0.8865 nsec

6. DISCUSSION OF RESULTS

The results obtained for IEMP problem 4 are presented in a graphical format starting with Figure 3 and continuing through Figure 22. The same information is displayed in a tabular format starting with Table 5 and ending with Table 14. Because of the extensive nature of the graphs and tables, they have been placed at the end of the report for easy reference.

No attempt will be made in this section to physically justify the results that are presented by an appeal to first principles. The intelligent comparison of the information presented with the experimental data gathered in the Benchmark Experiments will pass judgement on the reasonableness of the results. What will be presented here is a discussion of the results from a computational standpoint. This information may be of some use in helping the reader separate analytically induced errors from errors caused by inadequate physics.

The data points are plotted every 0.887 nsec out to 10.638 nsec and then four more points are included to extend the results out to 35.461 nsec. This particular choice of sample points was primarily dictated by economic (computing cost) considerations. It is intended to give the most information during the time frame where the most rapid variations in the results are expected. As a word of caution, it should be pointed out that the nonlinear spacing of the results presented does not imply a nonlinear spacing of the time step used in obtaining those results. The time step was held constant throughout the calculations at 0.887 nsec.

Another factor which should be commented on is the description of the spatial variation of the current distribution. As mentioned earlier, DYNACYL allows one to choose between a constant and a Gaussian variation in current density with respect to radius. Sample calculations were run using both descriptions.

It was noted that there was a very small difference in the results obtained using these two descriptions. That is, small in comparison to the magnitude of errors normally encountered in such calculations. This is not particularly surprising observation for this problem since the constant current distribution used 2.7 amp/cm^2 while the

Gaussian had a peak value of 3.12 amp/cm^2 and decreased to 2.08 amp/cm^2 at the cylinder wall. The results shown in this report were obtained using the Gaussian description, for the most part. However, all of the values associated with the last four time points were obtained using the constant current distribution. The author does not expect much more than a ± 5 percent difference between these values and those that would have been obtained using the Gaussian description.

It should be pointed out that not all of the variable values were calculated by DYNACYL at the particular point in space required by the problem description (dictated by location of sensors in the experiment). DYNACYL is constructed in such a way that some variables are computed at the boundary between spatial zones and some are calculated at the center of spatial zones. In computing the total space current, for example, DYNACYL calculates axial components of current density at the center of zones, while the radial components are computed at the boundaries between zones. Thus, interpolation between the radial components must be performed to obtain values at zone centers.

In other cases it was necessary to extrapolate from calculated data points. Such was the case with $H\phi$ since the zoning used did not yield values at $r = 13.8$ cm (the location of the measured field), but instead yielded values at $r = 12.775$ cm. The extrapolating was done using a power curve fit on the values calculated at 9.125 cm and 12.775 cm. The curve fitting was done on an HP-67 calculator using their standard curve fitting program.

In summary, the results presented possibly suffer from insufficient time domain sampling and in some cases insufficient spatial sampling. The factor should certainly be kept in mind in evaluating DYNACYL's capability.

7. RECOMMENDATIONS

The author's experience with DYNACYL has lead him to raise the following question: how much of DYNACYL's computational error can be assigned to inadequate treatment of air-ionization and how much of the error can be assigned to inadequate description of the incident beam? Unquestionably, both factors contribute to the error but experience has indicated that DYNACYL can be quite sensitive to variations in the beam energy description. The problem is compounded since part of DYNACYL's input data was generated by another computer program, ELTRAN.

A more detailed exercise of DYNACYL's characteristics would be a recalculation of IEMP problem 4 while varying several of the parameters, one at a time, that are used to describe incident beam energy. Such a study would allow one to speculate on percentage error in predicted results as a function of percentage error in the input data. One may find, for example, that the accuracy of DYNACYL's output may be severely limited by ones ability to describe the input. Secondly, the author suggests that DYNACYL be modified to allow variations in describing the distribution of the emitted particles with respect to angle. As it stands, DYNACYL allows for time variation in energy levels but not time variations in angular distribution. It is thought that such a modification may allow significant improvements in DYNACYL's capability to accurately predict results and pave the way to tackle the more difficult problem of air-ionization effects. It will be difficult to correct inadequate modeling of air chemistry until one is sure that other significant sources of error have been eliminated. In conclusion, the Benchmark Experiments could prove to be as useful in helping the community to improve their codes as it has been in helping the community find the weaknesses of their codes.

Table 5. Computed Values of $H\phi(t)$ at Constant r, Different Values of z. Field is Assumed Constant with Respect to ϕ.

	$H\phi(t)$				
r = 13.8 cm	P = 2 mtorr				
	z(cm)				
Time	0	2.5	17.5	32.5	50
0.887	-166.5	-159.4	-71.5	-13.5	0
1.773	-526.7	-372.4	-202.5	-40.7	0
2.660	-805.8	-746.3	-229.0	-56.9	-28.4
3.545	-1257.0	-1101.0	-457.0	-96.3	-117.0
4.433	-1420.0	-1218.0	-526.9	-196.3	-238.0
5.319	-1452.0	-1226.0	-521.0	-290.9	-315.0
6.206	-1315.0	-961.0	-492.0	-306.9	-230.0
7.092	-1022.0	-711.3	-535.0	-374.0	-106.8
7.979	-395.0	-293.0	-251.0	-91.4	-58.2
8.865	-600.0	-495.0	-232.0	-68.2	-84.5
9.752	-769.0	-663.0	-95.8	+18.0	-189.0
10.638	-416.0	-926.7	+57.4	+106.4	-80.8
17.731	-1030.0	-780.0	-194.3	-221.2	+41.3
26.596	+128.0	0	-43.6	-24.6	+55.0
35.461	-58.0	-53.2	-15.6	-2.6	-2.5

Table 6. Computed Values of $H\phi(t)$ at Constant r, Different Values of r. Field is Assumed Constant with Respect to ϕ.

	$H\phi(t)$				
r = 13.8 cm	P = 100 mtorr				
Time	0	2.5	17.5	32.5	50
0.887	-1.242^{2}	-1.122^{2}	-48.69	-10.62	-2.504^{-2}
1.773	-4.096^{2}	-3.695^{2}	-1.691^{2}	-33.96	-2.845^{-1}
2.660	-8.265^{2}	-7.372^{2}	-3.276^{2}	-58.26	-2.93^{1}
3.546	-1.202^{3}	-1.057^{3}	-4.987^{2}	-1.068^{2}	-1.96^{2}
4.433	-1.424^{3}	-1.235^{3}	-5.969^{2}	-2.159^{2}	-2.089^{2}
5.319	-1.5^{3}	-1.369^{3}	-6.610^{2}	-3.258^{2}	-2.747^{2}
6.206	-1.691^{3}	-1.4^{3}	-6.321^{2}	-3.584^{2}	-2.693^{2}
7.092	-1.512^{3}	-1.319^{3}	-5.254^{2}	-3.83^{2}	-2.525^{2}
7.979	-1.619^{3}	-1.34^{3}	-5.011^{2}	-4.016^{2}	-2.287^{2}
8.865	-1.832^{3}	-1.571^{3}	-5.461^{2}	-2.969^{2}	-1.786^{2}
9.752	-1.458^{3}	-1.261^{3}	-5.266^{2}	-3.323^{2}	-2.022^{2}
10.638	-1.597	-1.412^{3}	-5.576^{2}	-3.255^{2}	-2.006^{2}
17.731	-1.738^{3}	-1.568^{3}	-8.63^{2}	-5.101^{2}	-3.751^{2}
26.596	-8.549^{2}	-8.105^{2}	5.787^{2}	-3.8^{2}	-3.405^{2}
35.461	-5.642^{2}	-5.568^{2}	-4.45^{2}	-3.754^{2}	-3.153^{2}

Table 7. Computed Values of $H\phi(t)$ at Constant r, Different Values of z. Field is Assumed Constant with Respect to ϕ.

	$H\phi(t)$				
r = 13.8 cm	P = 300 mtorr				
	z(cm)				
Time	0	2.5	17.5	32.5	50
0.887	-1.233^{2}	-1.12^{2}	-41.97	-10.77	-2.511^{-2}
1.773	-3.911^{2}	-3.568^{2}	-1.383^{2}	-3.058^{1}	-0.3061
2.660	-7.364^{2}	-6.691^{2}	-2.624^{2}	-50.30	-2.358
3.546	-1.093^{3}	-9.741^{2}	-3.792^{2}	-1.29^{2}	-75.23
4.433	-1.335^{3}	-1.299^{3}	-4.736^{2}	-1.672^{2}	-1.133^{2}
5.319	-1.761^{3}	-1.588^{3}	-6.001^{2}	-2.637^{2}	-1.436^{2}
6.206	-1.886^{3}	-1.74^{3}	-8.283^{2}	-3.776^{2}	-1.854^{2}
7.092	-1.998^{3}	-1.84^{3}	-9.98^{2}	-5.319^{2}	-2.903^{2}
7.979	-1.937^{3}	-1.781^{3}	-1.055^{3}	-6.242^{2}	-4.133^{2}
8.865	-1.894^{3}	-1.741^{3}	-1.008^{3}	-6.698^{2}	-5.432^{2}
9.752	-1.804^{3}	-1.659^{3}	-9.975^{2}	-6.824^{2}	-4.516^{2}
10.638	-1.743^{3}	-1.599^{3}	-9.815^{2}	-6.931^{2}	-4.369^{2}
17.731	-1.794^{3}	-1.602^{3}	-8.676^{2}	-4.992^{2}	-3.047^{2}
26.596	-8.681^{2}	-8.168^{2}	-6.165^{2}	-4.008^{2}	-3.239^{2}
35.461	-6.448^{2}	-6.308^{2}	-0.4949^{2}	-4.000^{2}	-3.442^{2}

Table 8. Computed Values of Hϕ(t) at Constant r, Different Values of z. Field is Assumed Constant with Respect to ϕ.

		Hϕ(t)			
r = 13.8 cm		P = 50 mtorr			
Time	0	2.5	17.5	32.5	50
0.887	-132.2	-119.73	-48.4	-10.9	0
1.773	-428.4	-358.22	-160.59	-34.501	-12.1
2.660	-827.6	-736.7	-296.0	-55.74	-38.9
3.546	-1145	-998.8	-393.0	-100.2	-104.4
4.433	-1417.2	-1056.8	-482.8	-189.1	-186.9
5.319	-1760.8	-1519.2	-552.7	-244.3	-233.09
6.206	-1949.3	-1679.0	-595.9	-266.6	-205.6
7.092	-1954.3	-1700.7	-687.0	-285.3	-139.4
7.979	-1852.9	-1627.1	-746.0	-325.1	-151.2
8.865	-1773.6	-1554.5	-765.0	-438.7	-206.0
9.752	-1608.1	-1419.1	-719.8	-409.9	-274.2
10.638	-1558.0	-1377.3	-709.9	-439.8	-225.9
17.731	-1123.4	-934.7	-349.0	-174.3	-65.7
26.596	-524.1	-491.5	-210.4	-49.0	-12.71
35.461	-440.7	-394.0	-156.9	-38.12	-10.686

Table 9. Total Space Current at Different Values of z

Time (nsec)	Total Current $I_t(t)$, P = 2 mtorr, z(cm): 0	5	30	35	55
0.887	-147.73	-108.71	0	0	0
1.773	-388.83	-290.73	-17.12	-0.971	0
2.660	-745.12	-550.9	-65.95	-28.9	0
3.546	-1041.15	-759.7	-274.9	-87.8	-10.5
4.433	-1221.1	-855.1	-214.0	-185.4	-43.5
5.319	-1304.7	-842.5	-286.3	-272.29	-160.14
6.206	-1408	-748.9	-281.5	-251.9	-166.8
7.092	-840	-492.9	-304.4	-242.75	-162.76
7.979	-587.3	-344.95	-251.4	-186.39	-120.98
8.865	-775.1	-272.5	-96.68	-92.2	-77.7
9.752	-551.0	-463.42	-47.57	-36.4	-71.3
10.638	-458.6	-222.0	-42.33	-45.0	-35.8
17.731	-861.3	-362.8	-75.85	-72.78	-36.9
25.596	+64.56	-38.95	-21.93	-15.23	-18.14
35.461	-50.9	-48.8	-1.394	0	0

Table 10. Total Space Current at Different Values of z

Time (nsec)	Total Current $I_t(t)$, P = 100 mtorr, z(cm) 0	5	30	35	55
0.887	-149.0	-108.0	0	0	0
1.773	-368.35	-281.6	-28.44	-1.7	0
2.660	-710.17	-530.3	-59.02	-23.7	0
3.546	-1002.6	-746.8	-162.9	-93.58	-13.53
4.433	-1207.3	-879.6	-258.9	-203.92	-48.49
5.319	-1307.8	-1042.3	-329.11	-285.5	-130.63
6.206	-1406.5	-1081.7	-333.4	-313.64	-266.68
7.092	-1312.7	-1003.7	-416.8	-345.79	-306.8
7.979	-725.02	-1100.4	-363.01	-275.72	-258.16
8.865	-1435.4	-1381.27	-376.6	-227.6	-191.3
9.752	-1182.7	-1095.7	-360.17	-293.81	-173.9
10.638	-1516.2	-1392.9	-389.9	-225.9	-150.1
17.731	-1421.4	-1205.6	-500.5	-445.6	-339.5
26.596	-812.56	-730.6	-450.8	-398.6	-322.01
35.461	-555.9	-38.0	-365.0	-330.0	-255.7

Table 11. Total Space Current at Different Values of z

	Total Current $I_t(t)$ P = 300 mtorr				
Time (nsec)	z(cm) 0	5	30	35	55
0.887	-147.8	-108.9	0	0	0
1.773	-205.05	-281.7	-17.1	-1.0	0
2.660	-623.9	-530.21	-74.35	-35.4	0
3.546	-898.8	-758.8	-160.34	-100.39	-13.96
4.433	-1171.2	-1077.6	-268.13	-179.6	-50.98
5.319	-1494.1	-1356.7	-343.6	-260.7	-113.56
6.206	-1451.2	-1512.0	-457.1	-342.1	-176.2
7.092	-1714.6	-1470.1	-574.3	-460.6	-219.8
7.979	-1731.8	-2444.8	-676.4	-598.5	-368.5
8.86	-1567.5	-1981.3	-675.3	-577.3	-372.1
9.752	-1501.9	-1360.3	-554.9	-627.9	-420.3
10.638	-1355.1	-1177.1	-631.0	-519.3	-295.2
17.731	-1444.7	-1254.5	-580.3	-452.6	-280.5
26.596	-824.3	-765.9	-454.8	-387.9	-293.0
35.641	-597.1	-582.4	-331.5	-333.1	-308.7

Table 12. Total Space Current at Different Values of z

Time (nsec)	Total Current $I_t(t)$, P = 50 mtorr, z(cm): 0	5	30	35	55
0.887	-139.78	-108.636	0	0	0
1.773	-359.4	-285.65	-16.64	0	0
2.660	-641.27	-521.85	-65.39	-28.073	0.10
3.546	-809.47	-695.4	-149.36	-87.25	-10.648
4.443	-1082.1	-867.4	-226.26	-170.5	-42.517
5.319	-1373.7	-1116.7	-278.0	-235.2	-170.6
6.206	-1080.3	-1242.8	-325.9	-257.45	-156.2
7.092	-1483.9	-1034.07	-378.0	-303.24	-127.1
7.979	-1423.0	-1238.9	-425.2	-328.31	-166.3
8.865	-1353.6	-1188.8	-470.7	-351.9	-188.32
9.752	-1244.8	-1108.3	-401.9	-349.7	-249.8
10.638	-1173.14	-1075.9	-256.4	-346.16	-322.59
17.731	-926.6	-724.0	-288.8	-138.9	-92.51
26.596	-485.1	-444.5	-70.8	-38.32	-10.4
35.461	-416.75	-355.6	-37.10	-27.12	-9.8

Table 13. Computed Values of End Plate Current, Axial and Radial E Fields At a Pressure of 2 mtorr and 100 mtorr

		$I_r(t)$ (amps) r(cm)				$E_z(t)$ (volts/m) at r=0 (cm) z(cm)			$E_r(t)$ (volts/m) at r=14.6 (cm) z(cm)	
	Time	r≤3.8	r≤7.6	r≤11.6	r≤14.6	0	32.5	55	2.5	50
2 mtorr	0.887	0	0	0	0	5.517^{+4}	-4.297^{+3}	-8.120^{-2}	-1.991^{+4}	-1.100^{+1}
	1.773	0	0	0	0	2.305^{+5}	-2.175^{+4}	-4.976^{+3}	-6.059^{+4}	-7.640^{+2}
	2.660	0	0	0	0	6.697^{+5}	-7.109^{+4}	-3.770^{+4}	-1.237^{+5}	-9.470^{+3}
	3.546	0	0	0	0	1.243^{+6}	-9.906^{+4}	-1.176^{+5}	-1.755^{+5}	-2.954^{+4}
	4.433	2.13	3.89	5.26	5.85	2.058^{+6}	-2.137^{+5}	-2.248^{+5}	-2.162^{+5}	-6.873^{+4}
	5.319	5.38	9.19	1.727^{1}	1.935^{1}	1.594^{+6}	-1.659^{+5}	-1.245^{+5}	-2.986^{+5}	-1.167^{+5}
	6.206	1.027^{1}	3.315^{1}	7.804^{1}	8.206^{1}	2.196^{+6}	-1.440^{+5}	-1.681^{+5}	-3.917^{+5}	-1.298^{+5}
	7.092	1.30^{-1}	2.045^{1}	7.214^{1}	9.206^{1}	1.938^{+6}	-3.412^{+4}	-4.375^{+4}	-4.718^{+4}	-6.759^{+4}
	7.979	1.380^{1}	3.268^{1}	6.206^{1}	1.241^{2}	1.257^{+6}	$+8.681^{+4}$	-1.798^{+5}	-6.518^{+5}	-2.170^{+4}
	8.865	0	1.409^{1}	5.678^{1}	6.792^{1}	1.242^{+6}	-3.039^{+4}	-1.253^{+5}	-6.384^{+5}	-2.328^{+4}
	9.752	0	0	3.057^{1}	5.532^{1}	1.036^{+6}	-2.284^{+4}	9.728^{+4}	-5.342^{+5}	-2.822^{+4}
	10.638	0	4.564^{1}	6.250^{1}	6.518^{1}	7.414^{+5}	-2.776^{+4}	-2.216^{+5}	-5.760^{+5}	-3.497^{+4}
	17.731	0	0	0	0	1.341^{+6}	$+1.650^{+3}$	-7.672^{+4}	-1.260^{+6}	-2.684^{+4}
	26.596	0	0	0	0	-1.101	-2.330^{+2}	-1.524^{+2}	-1.524^{+2}	+2.451
100 mtorr	0.887	0	0	0	0	5.056^{+4}	-4.204^{+3}	-7.959^{-2}	-2.048^{+4}	-1.102^{1}
	1.773	0	0	0	0	2.020^{+5}	-2.020^{+4}	-4.751^{+3}	-5.907^{+4}	-7.304^{2}
	2.660	0	0	0	0	5.674^{+5}	-5.949^{+4}	-3.479^{+4}	-1.148^{+5}	-9.833^{3}
	3.546	0	0	0	0	9.834^{+5}	-8.631^{+4}	-9.524^{+4}	-1.595^{+5}	-2.906^{+4}
	6.206	2.148^{-4}	3.910^{-4}	5.296^{-4}	5.870^{-4}	1.246^{+6}	-1.444^{+5}	-2.044^{+5}	-1.928^{+5}	-6.128^{+4}
	5.319	7.739^{-4}	8.893^{-4}	1.689^{-3}	1.826^{-3}	1.835^{+6}	-1.097^{+5}	-2.216^{+5}	-2.288^{+5}	-9.007^{+4}
	6.206	8.103^{-4}	3.475^{-3}	5.745^{-3}	6.765^{-3}	1.513^{+6}	-1.139^{+5}	-1.168^{+5}	-2.611^{+5}	-8.098^{+4}
	7.092	1.255^{-3}	3.355^{-3}	1.040^{-2}	1.269^{-2}	1.429^{+6}	-3.259^{+4}	-2.376^{+5}	-2.583^{+5}	-5.634^{+4}
	7.979	1.366^{-3}	5.606^{-3}	1.021^{-2}	1.148^{-2}	1.449^{+6}	8.025^{3}	-1.069^{+5}	-6.566^{+5}	-4.025^{+4}
	8.865	5.981^{-4}	8.349^{-3}	1.329^{-2}	1.360^{-2}	6.244^{+5}	-6.235^{4}	-1.284^{+5}	-1.472^{+5}	-1.157^{+4}
	9.752	1.089^{-4}	4.323^{-3}	7.449^{-3}	7.706^{-3}	-5.733^{+3}	6.277^{+4}	-7.100^{+4}	-1.133^{+5}	-8.527^{+4}
	10.638	1.512^{-3}	6.263^{-3}	1.034^{-2}	1.037^{-2}	7.121^{+4}	-9.035^{+4}	-1.315^{+5}	-9.152^{+3}	-6.111^{+3}
	17.731	2.575^{-3}	4.835^{-3}	8.966^{-3}	1.165^{-2}	1.222^{+3}	4.144^{+3}	-1.207^{+4}	-6.181^{+3}	-8.461^{+3}
	26.596	3.831^{-3}	6.033^{-6}	8.678^{-3}	1.133^{-2}	-3.515^{+2}	-3.983^{+3}	-3.862^{+3}	$+1.820^{+3}$	-2.756^{+3}
	35.461	9.526^{-4}	4.426^{-3}	6.744^{-3}	6.837^{-3}	-8.230^{+3}	-1.269^{+3}	-5.324^{+2}	$+2.024^{+2}$	-1.245^{+4}

Table 14. Computed Values of End Plate Current, Axial and Radial E Fields At a Pressure of 300 mtorr and 50 torr

		$I_r(t)$ (amps) r(cm)				$E_z(t)$ (volts/m) at r=0 (cm) z(cm)			$E_r(t)$ (volts/m) at r=14.6 (cm) z(cm)	
	Time	$r\le3.8$	$r\le7.6$	$r\le11.6$	$r\ge14.6$	0	32.5	55	2.5	50
300 mtorr	0.887	0	0	0	0	4.818^{+4}	-4.243^{+3}	-8.110^{-2}	-2.086^{+4}	-1.104^{+1}
	1.773	0	0	0	0	1.522^{+5}	-1.979^{+4}	-4.727^{+3}	-5.448^{+4}	-5.481^{+2}
	2.660	0	0	0	0	3.132^{+5}	-4.323^{+4}	-3.259^{+4}	-9.146^{+4}	-7.838^{+3}
	3.546	0	0	0	0	3.922^{+5}	-3.943^{+4}	-7.549^{+4}	-9.004^{+4}	-2.375^{+4}
	4.433	2.18	4.010	5.380	5.970	2.746^{+5}	-1.164^{+5}	-5.189^{+4}	-6.639^{+4}	-4.018^{+4}
	5.319	7.09	1.520^{1}	1.929^{1}	1.998^{1}	2.115^{+5}	-1.064^{+4}	-8.738^{+4}	-5.851^{+4}	-3.580^{+4}
	6.206	1.354^{1}	3.433^{1}	4.305^{1}	4.483^{1}	2.864^{+5}	$+7.955^{+3}$	-4.956^{+4}	-2.981^{+4}	-2.771^{+3}
	7.092	1.330^{1}	4.224^{1}	6.803^{1}	8.108^{1}	2.881^{+4}	-1.739^{+4}	-6.532^{+4}	-3.534^{+4}	-5.144^{+4}
	7.979	2.263^{1}	3.019^{1}	4.964^{1}	7.329^{1}	3.985^{+5}	$+2.469^{+4}$	$+2.500^{+4}$	-2.415^{+4}	-6.691^{+3}
	8.865	1.148^{1}	9.662^{1}	1.742^{2}	2.866^{2}	4.196^{+4}	$+1.861^{+4}$	-8.373^{+4}	-3.405^{+4}	-2.619^{+4}
	9.752	1.218^{1}	5.153^{1}	1.028^{2}	1.307^{2}	1.050^{+4}	-8.720^{+3}	-4.203^{+4}	-7.246^{+3}	$+1.672^{+4}$
	10.638	4.437^{1}	9.287^{1}	1.736^{2}	2.2201^{2}	$+3.710^{+4}$	-6.192^{+3}	-3.616^{+4}	-1.943^{+4}	-3.288^{+4}
	17.731	2.909^{1}	5.832^{1}	6.513^{1}	6.938^{1}	2.273^{+4}	-2.883^{+3}	-1.660^{+4}	-5.035^{+3}	-8.090^{+2}
	26.596	2.864^{1}	7.753^{1}	1.076^{2}	1.153^{2}	-6.262^{+3}	-1.895^{+3}	-2.193^{+3}	$+1.520^{+3}$	-3.002^{+3}
	35.461	4.960	2.196^{1}	6.279^{1}	8.519^{1}	-4.494^{+3}	-1.775^{+3}	-1.366^{+3}	-4.131^{+1}	-5.216^{+3}
50 torr	0.887	0	0	0	0	4.190^{+4}	-4.262^{+3}	-7.76^{+2}	-1.6398^{+4}	-9.214
	1.773	0	0	0	0	1.738^{+5}	-2.168^{+4}	-4.846^{+3}	-4.6478^{+4}	-6.773^{+2}
	2.660	0	0	0	0	4.131^{+5}	-6.618^{+4}	3.492^{+4}	-8.745^{+4}	-8.895^{+3}
	3.546	0	0	0	0	3.991^{+5}	-8.606^{+4}	-1.035^{+5}	-1.080^{+5}	-2.805^{+4}
	4.433	1.480	3.320	4.700	5.270	1.780^{+5}	-1.258^{+5}	-2.123^{+5}	-1.145^{+5}	-5.727^{+4}
	5.319	5.940	1.132^{1}	1.899^{1}	2.117^{1}	1.631^{+5}	-4.670^{+4}	-1.511^{+5}	-1.145^{+5}	-8.893^{+4}
	6.206	1.627^{1}	3.209^{1}	6.170^{1}	7.295^{1}	1.712^{+5}	-4.166^{+4}	-1.546^{+5}	-5.123^{+4}	-8.731^{+4}
	7.092	1.228^{1}	3.178^{1}	8.341^{1}	9.941^{1}	9.329^{+4}	$+1.231^{+4}$	-1.856^{+5}	-4.700^{+4}	-5.572^{+4}
	7.979	9.620	3.964^{1}	5.908^{1}	6.306^{1}	5.217^{+4}	$+1.011^{+4}$	-2.246^{+5}	-2.567^{+4}	-6.026^{+4}
	8.865	1.043^{1}	5.024^{1}	5.861^{1}	7.053^{1}	3.763^{+4}	$+1.134^{+5}$	-1.972^{+5}	-1.107^{+4}	-3.660^{+4}
	9.752	1.450^{1}	3.392^{1}	5.190^{1}	5.446^{1}	2.788^{+4}	-1.327^{+4}	-2.115^{+5}	-3.816^{+3}	-6.894^{+4}
	10.638	1.502^{1}	9.290^{1}	1.071^{2}	1.084^{2}	2.022^{+4}	-1.199^{+4}	-3.576^{+4}	-3.474^{+3}	-4.337^{+4}
	17.731	7.060	1.647	1.716	2.017	1.445^{+3}	-5.163^{+3}	-2.187^{+2}	-6.489^{+3}	-4.046^{+2}
	26.596	2.400	2.900	2.900	2.900	-1.152^{+3}	-7.845^{+2}	-4.469^{+1}	-6.752^{+2}	-1.340^{1}
	35.461	0	0	0	0	-1.051^{+3}	-7.090^{+2}	-2.874^{+1}	-2.745^{+2}	-5.000

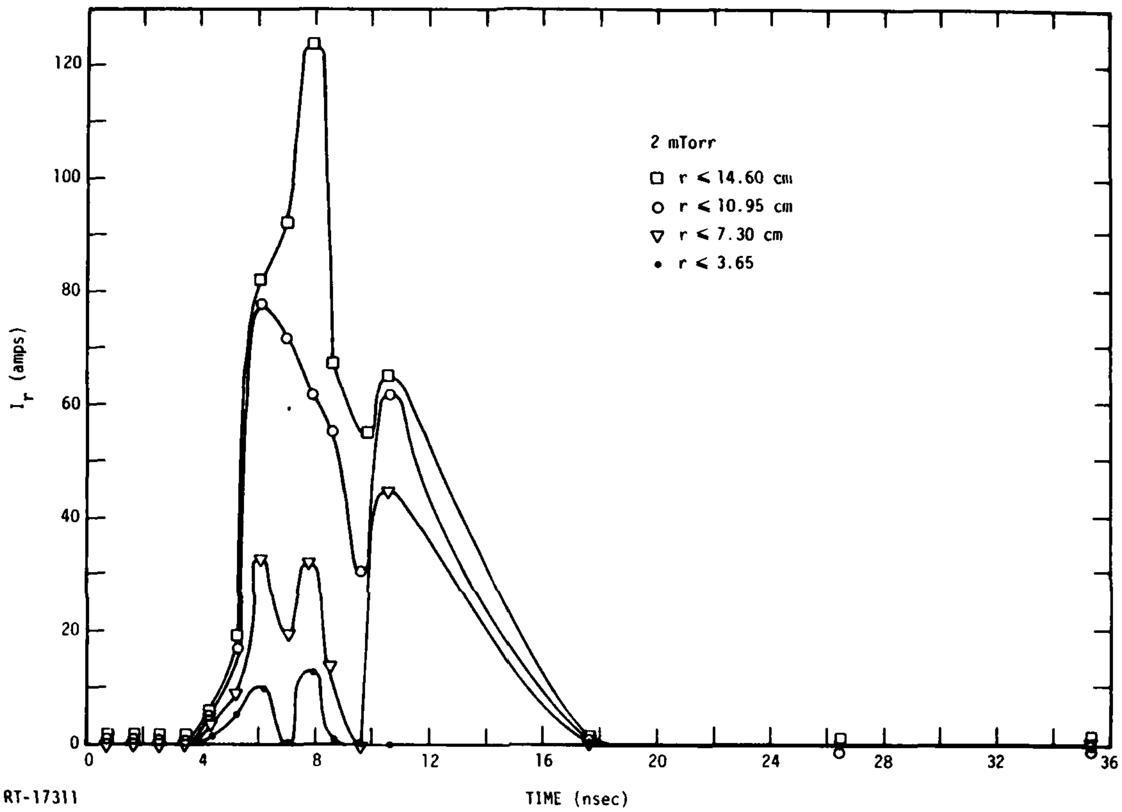

Figure 3. Radial current $I_r(t)$ on the end plate at z = 55 cm for different values of r at a pressure of 2 mtorr.

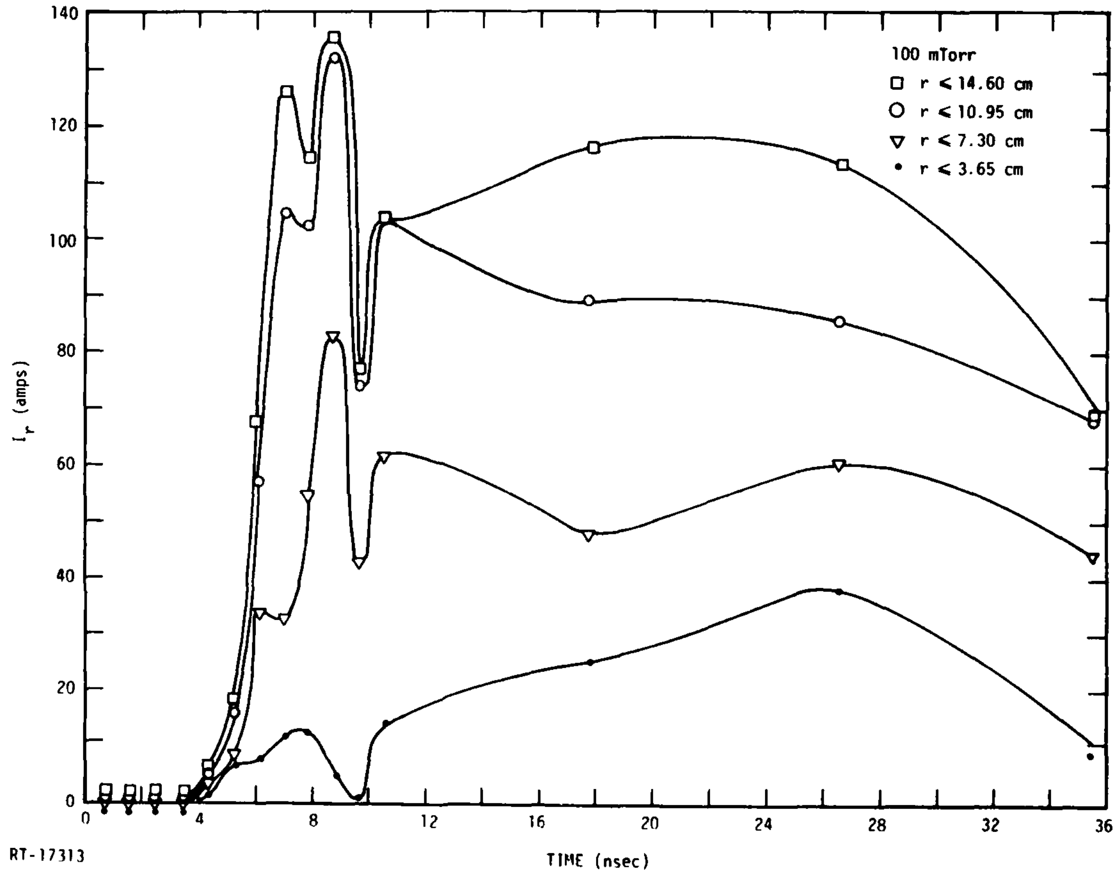

Figure 4. Radial current $I_r(t)$ on the end plate at z = 55 cm for different values of r at a pressure of 100 mtorr.

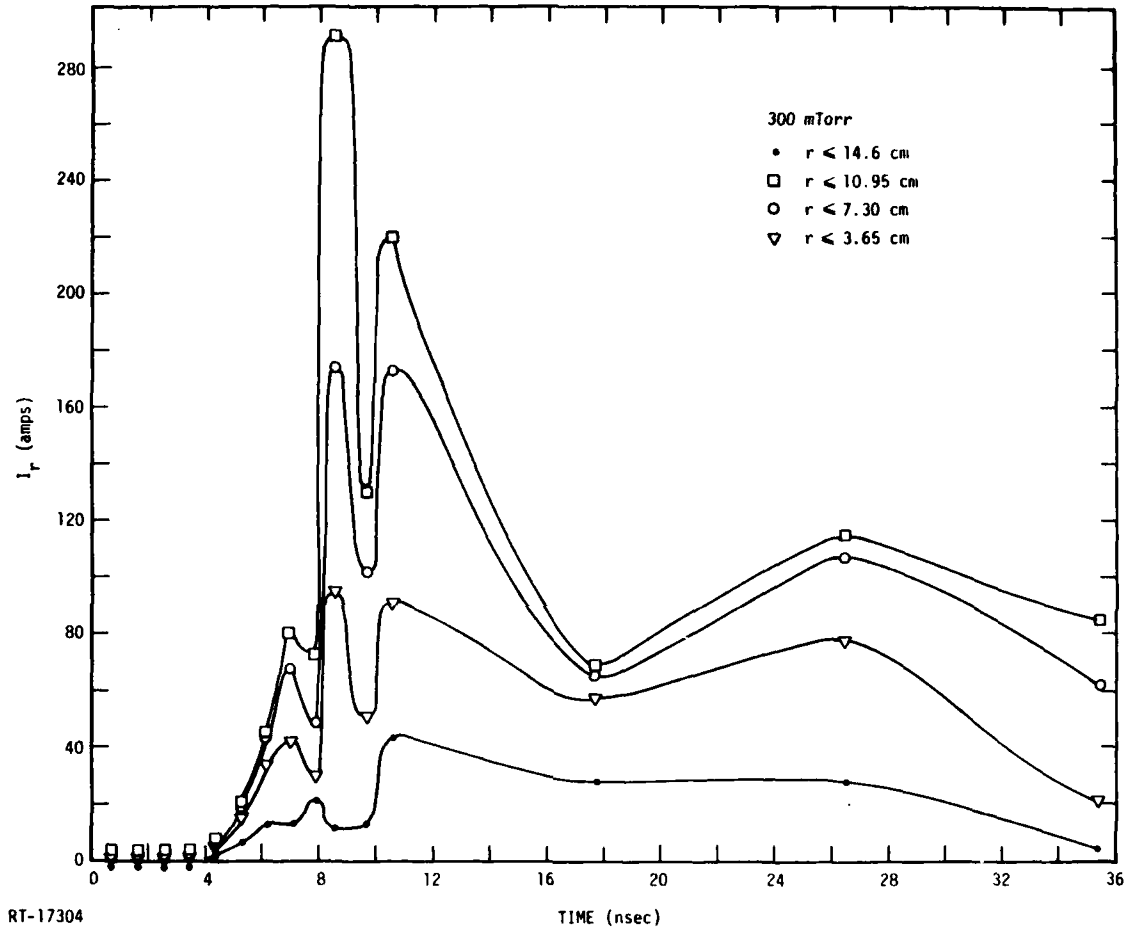

Figure 5. Radial current $I_r(t)$ on the end plate at z = 55 cm for different values of r at a pressure of 300 mtorr.

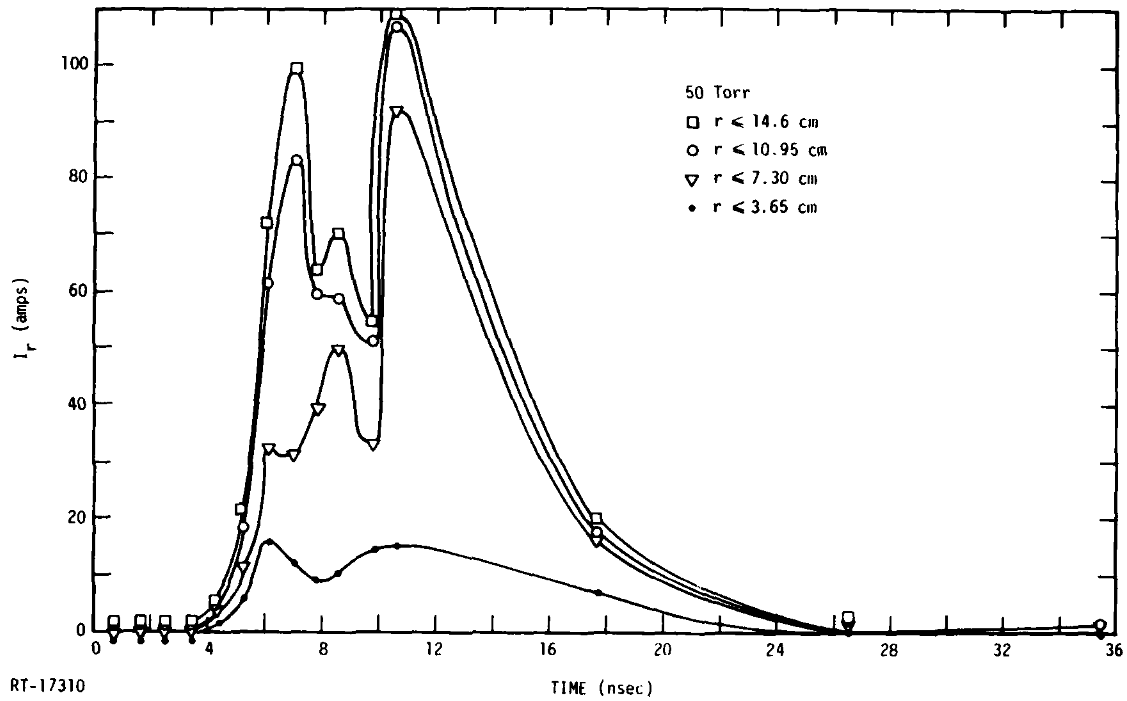

Figure 6. Radial current $I_r(t)$ on the end plate at z = 55 cm for different values of r at a pressure of 50 torr.

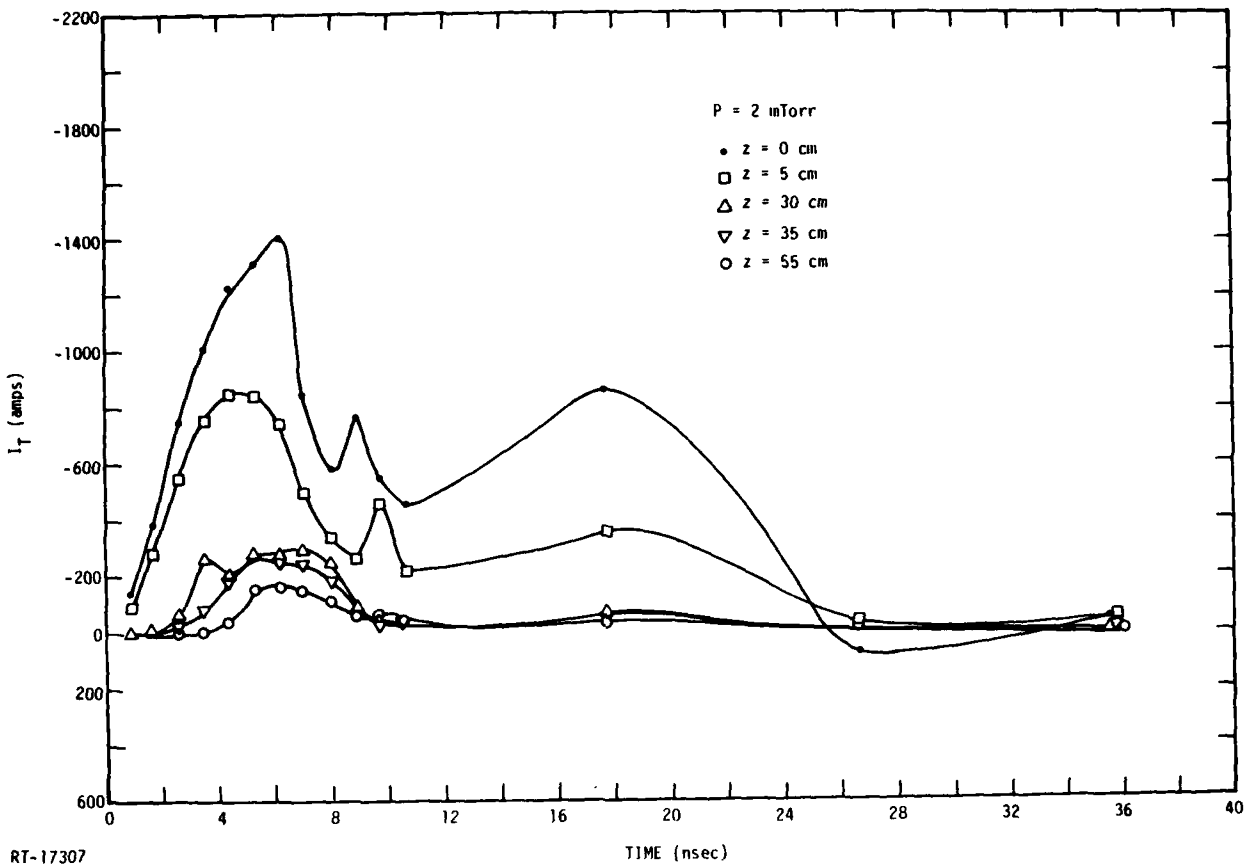

Figure 7. Total space current $I_t(t)$ at five different values of z at a pressure of 2 mtorr.

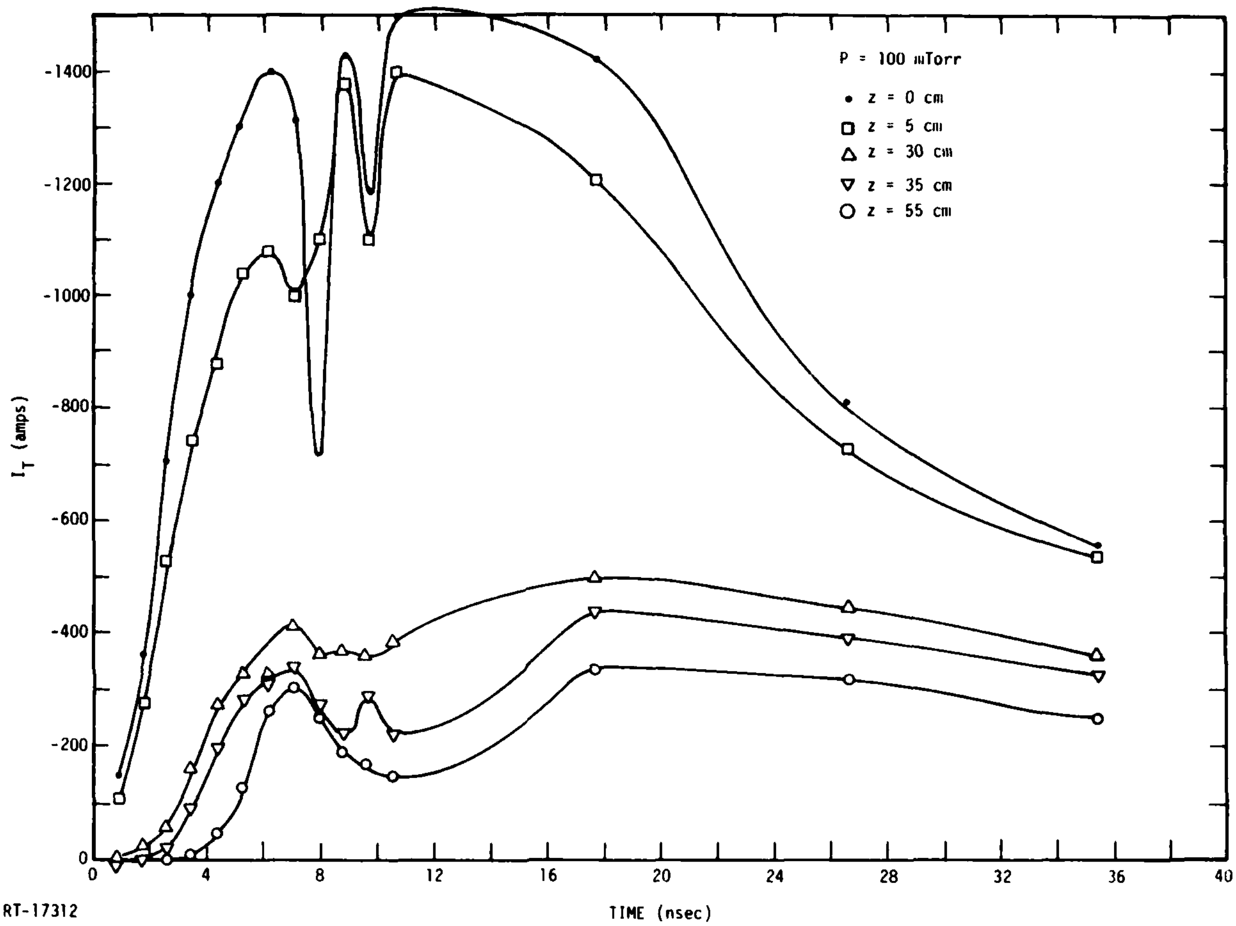

Figure 8. Total space current $I_t(t)$ at five different values of z at a pressure of 100 mtorr.

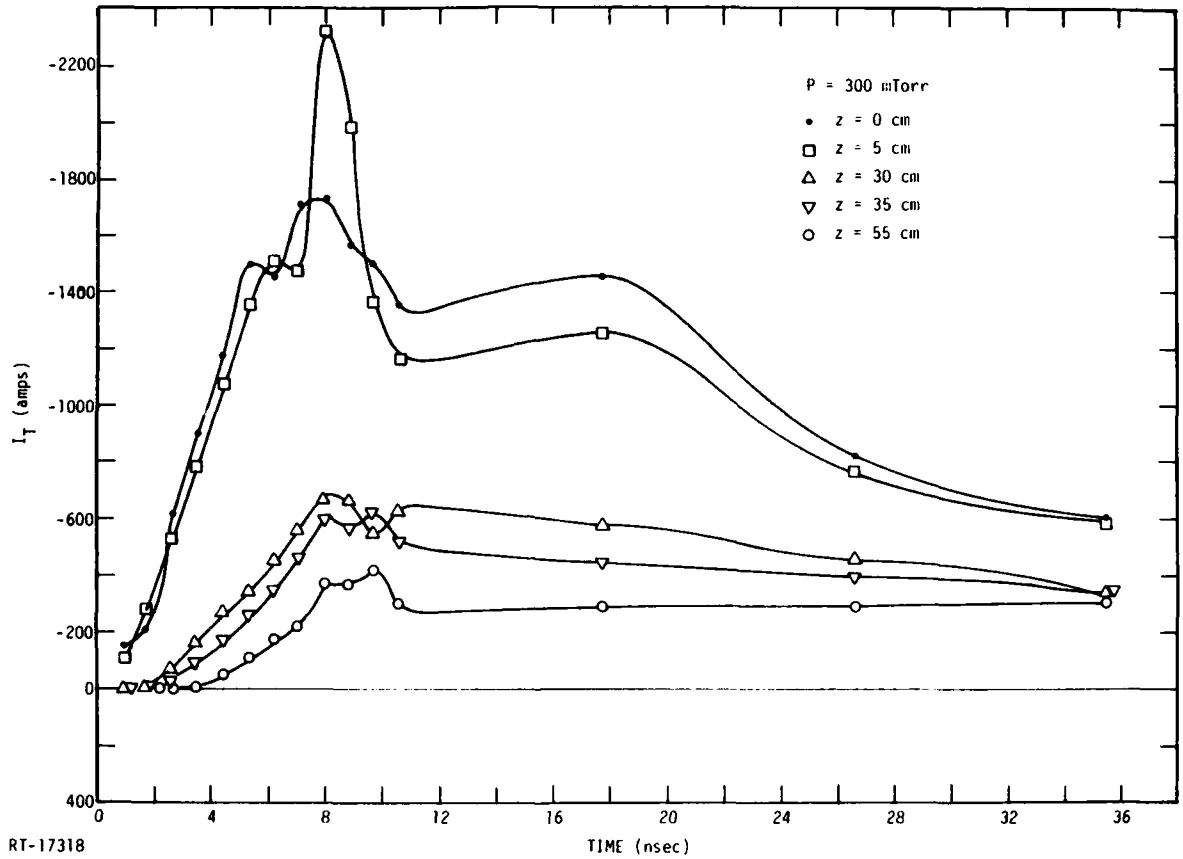

Figure 9. Total space current $I_t(t)$ at five different values of z at a pressure of 300 mtorr.

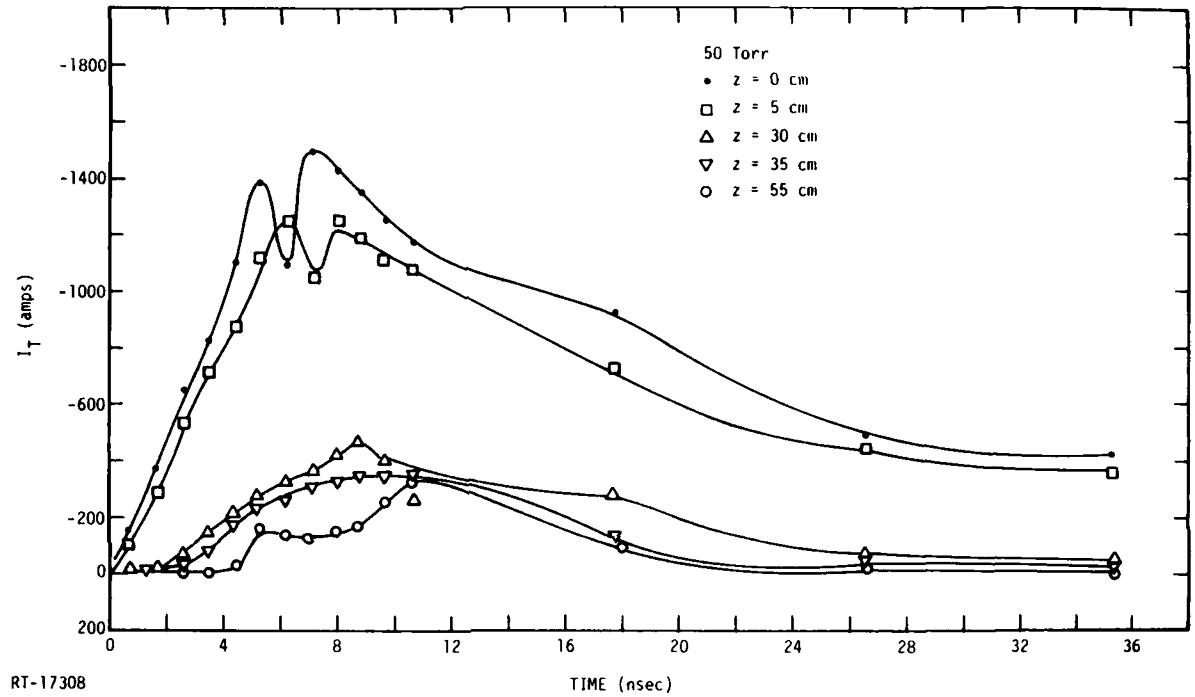

Figure 10. Total space current $I_t(t)$ at five different values of z at a pressure of 50 torr.

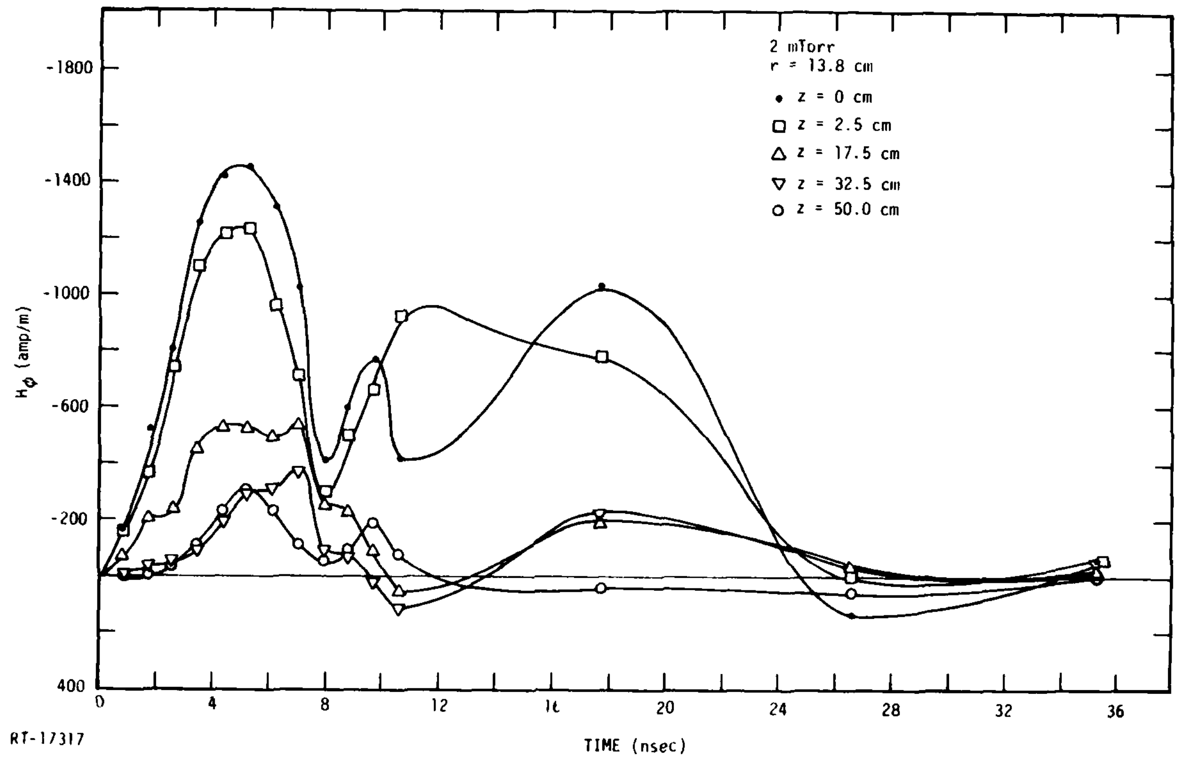

Figure 11. $H\phi(t)$ evaluated at r = 13.8 cm for five different values of z at a pressure of 2 mtorr. Variable is assumed constant with respect to ϕ.

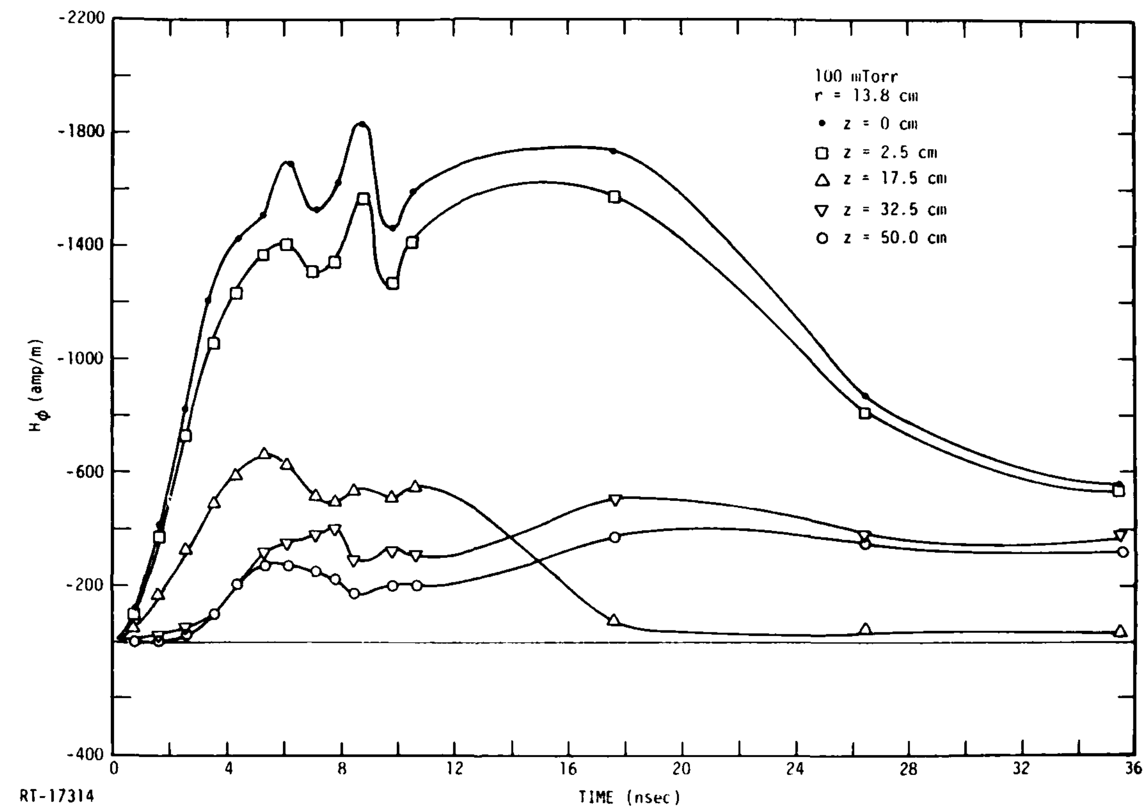

Figure 12. $H_\phi(t)$ evaluated at r = 13.8 cm for five different values of z at a pressure of 100 mtorr. Variable is assumed constant with respect to ϕ.

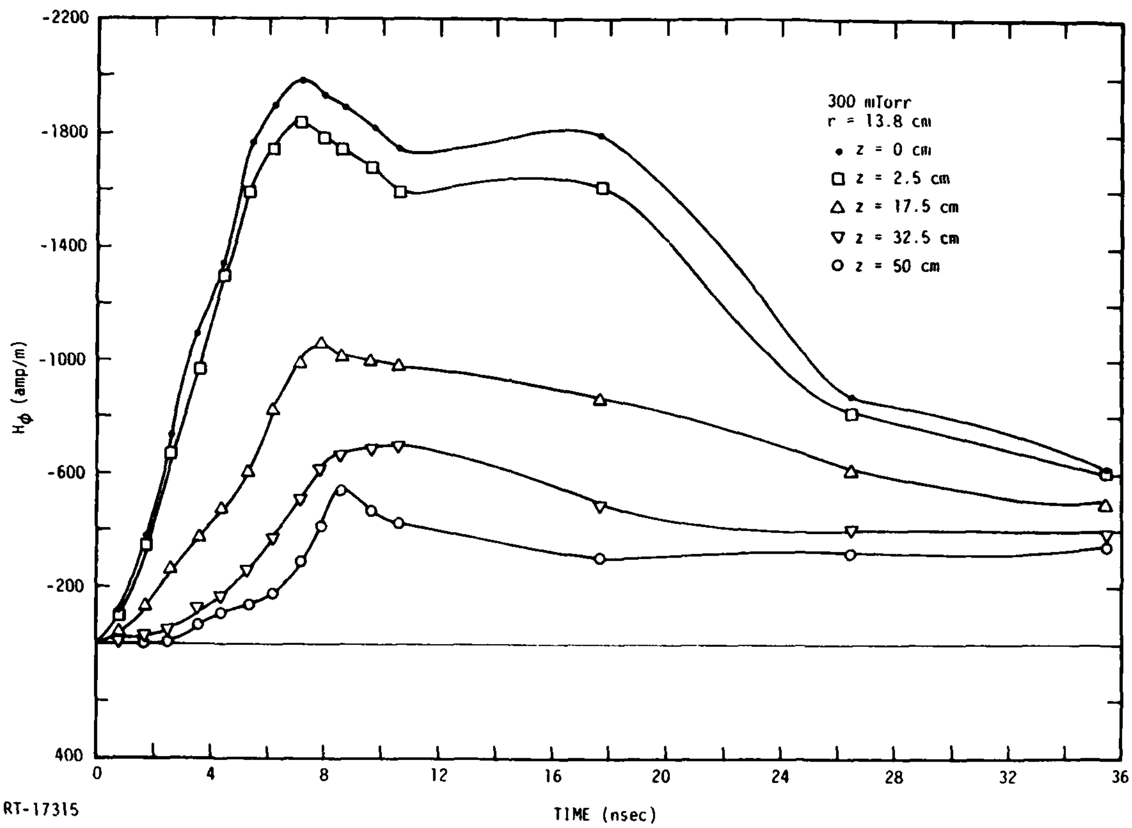

Figure 13. $H\phi(t)$ evaluated at $r = 13.8$ cm for five different values of z at a pressure of 300 mtorr. Variable is assumed constant with respect to ϕ.

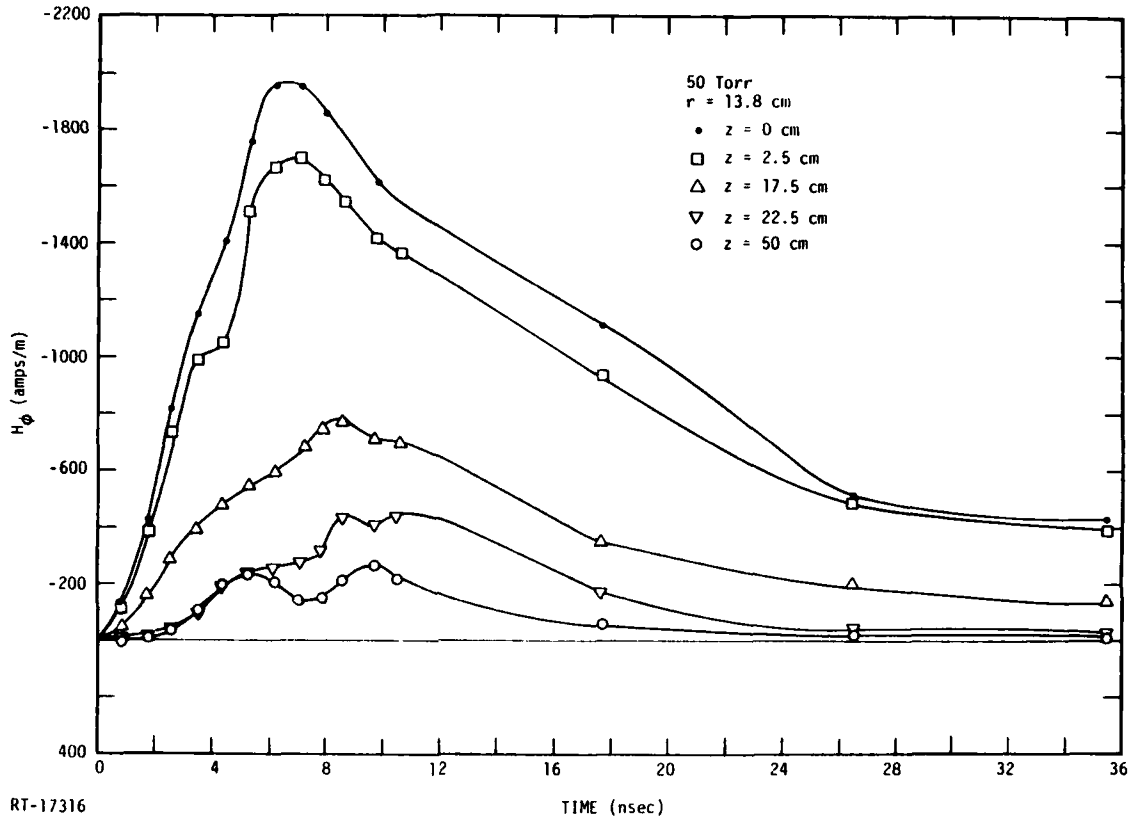

Figure 14. $H_\phi(t)$ evaluated at r = 13.8 cm for five different values of z at a pressure of 50 torr. Variable is assumed constant with respect to ϕ.

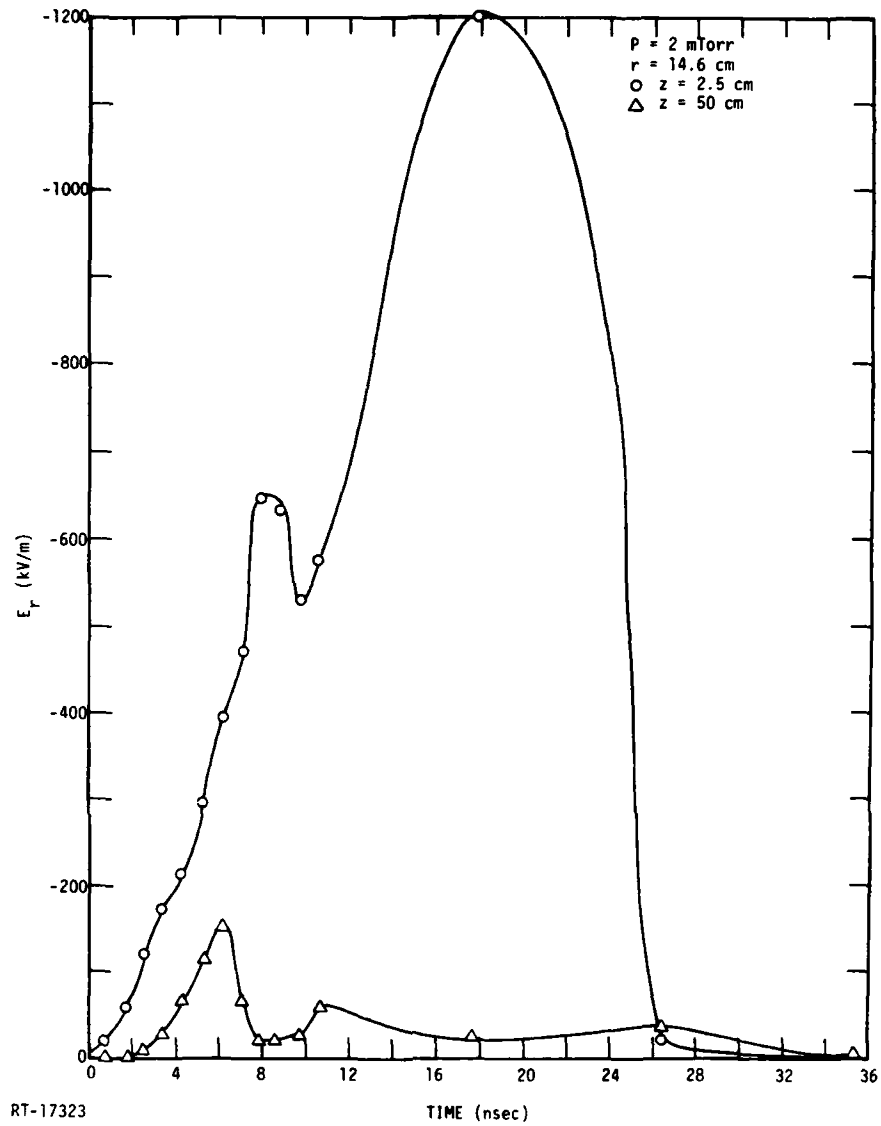

Figure 15. $E_r(t)$ at z = 2.5, 50 cm; r = 14.6 cm and a pressure of 2 mtorr.

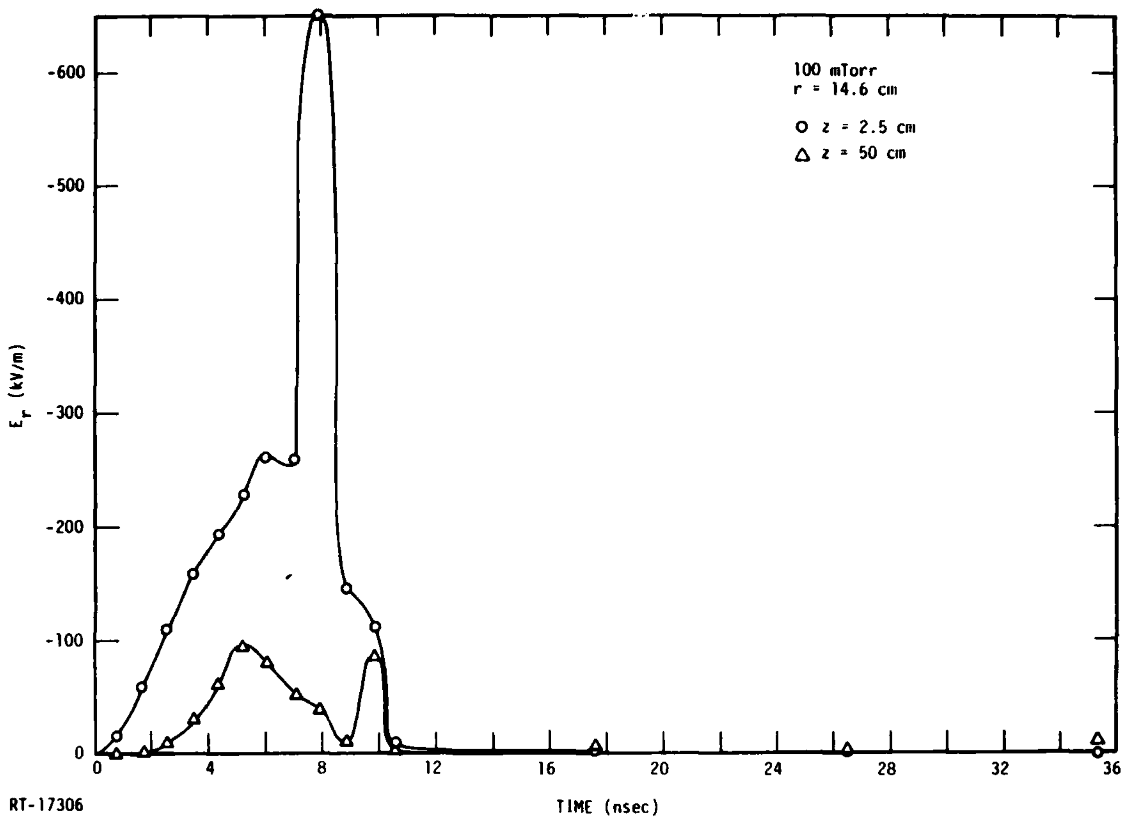

Figure 16. $E_r(t)$ at z = 2.5, 50 cm; r = 14.6 cm and a pressure of 100 mtorr.

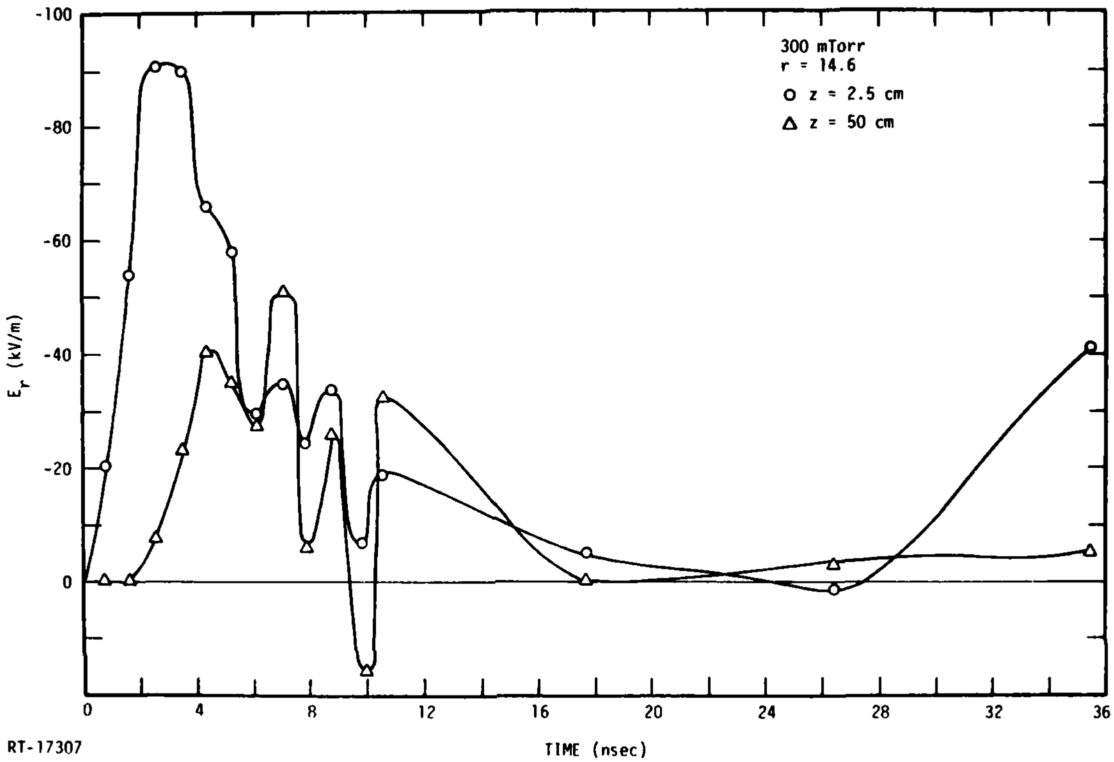

Figure 17. $E_r(t)$ at z = 3.5, 50 cm; r = 14.6 cm and a pressure of 300 mtorr.

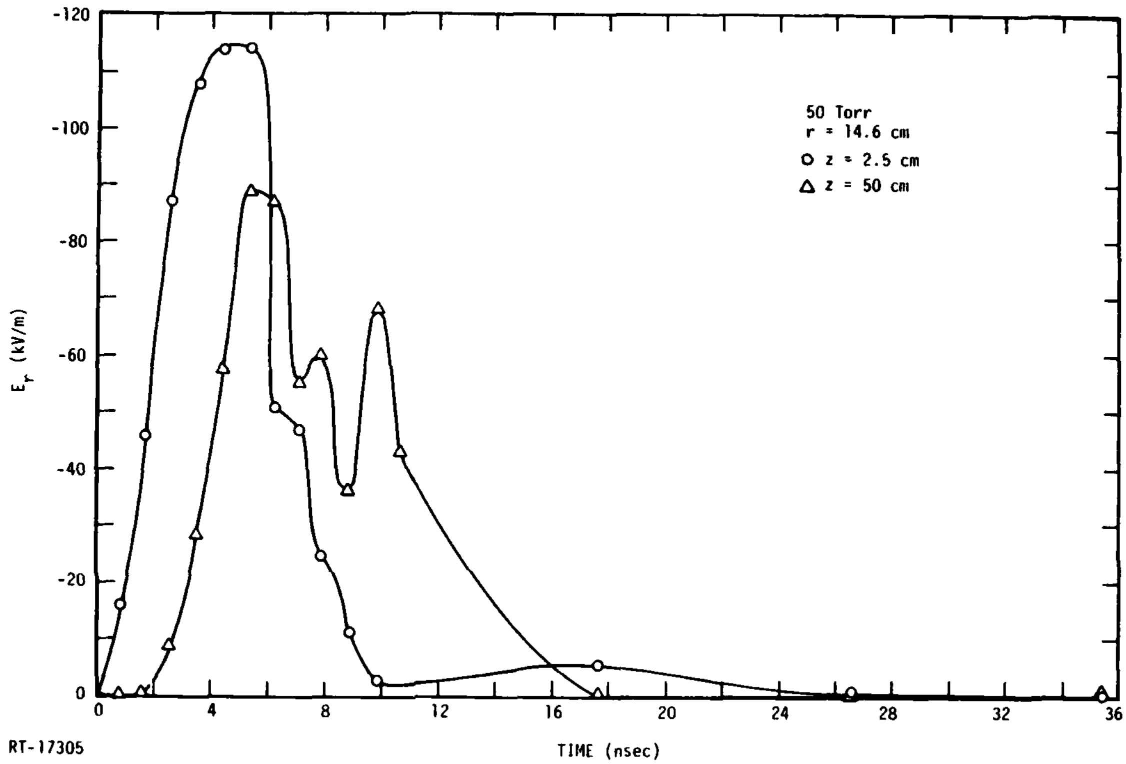

Figure 18. $E_r(t)$ at z = 2.5, 50 cm; r = 14.6 cm and a pressure of 50 torr.

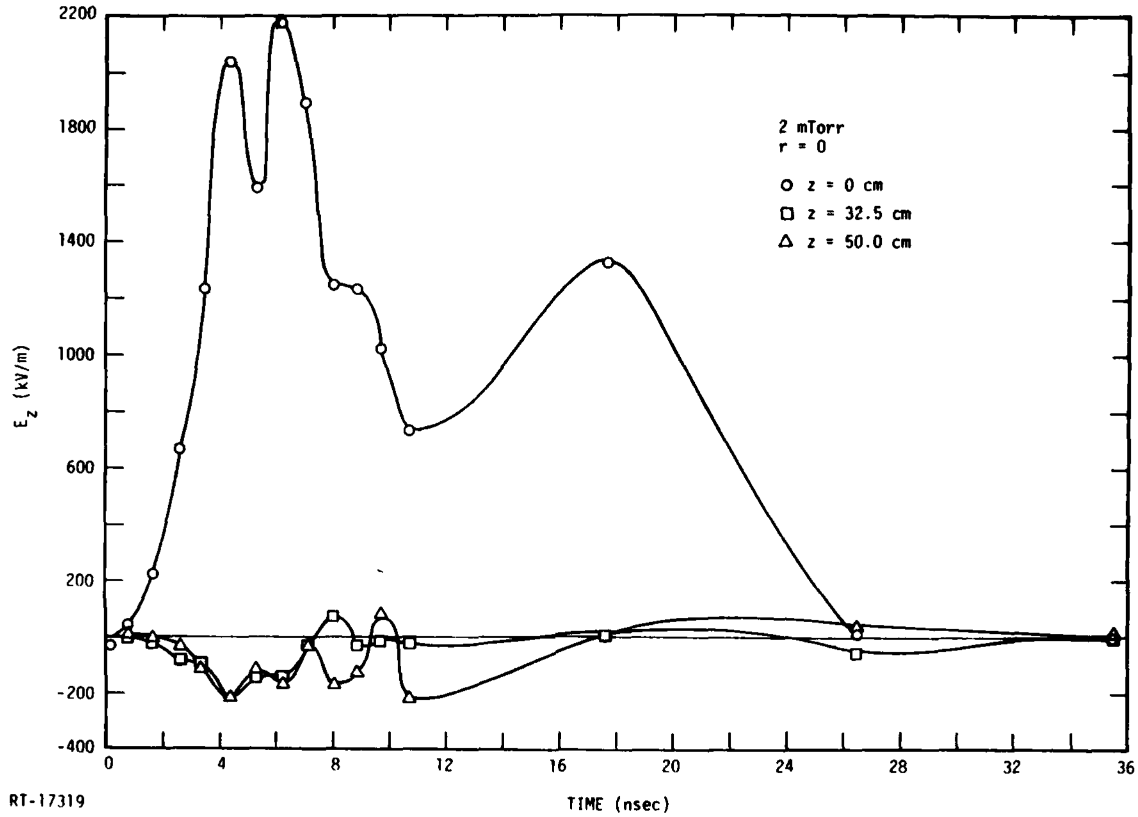

Figure 19. $E_z(t)$ at z = 0, 32.5, and 55 cm; r = 0 cm and a pressure of 2 mtorr.

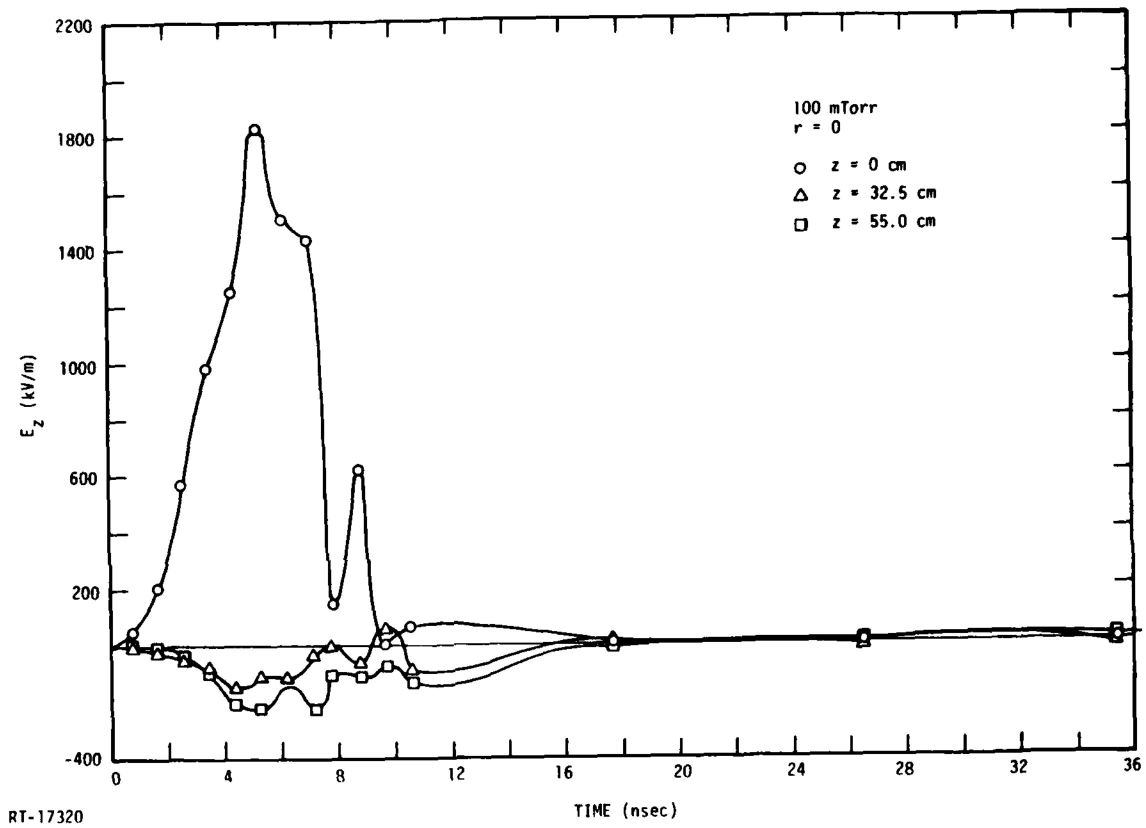

Figure 20. $E_z(t)$ at z = 0, 32.5, and 55 cm; r = 0 and a pressure of 100 mtorr.

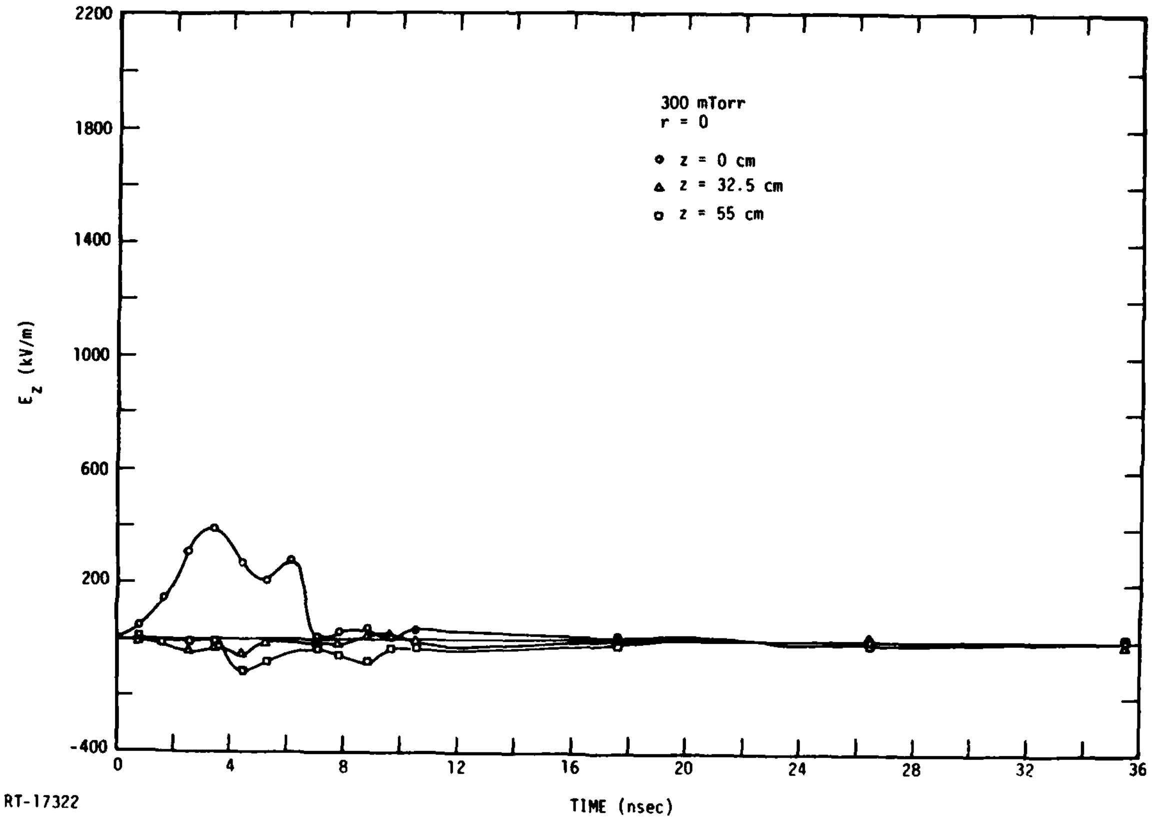

Figure 21. $E_z(t)$ at z = 0, 32.5, and 55 cm; r = 0 and a pressure of 300 mtorr.

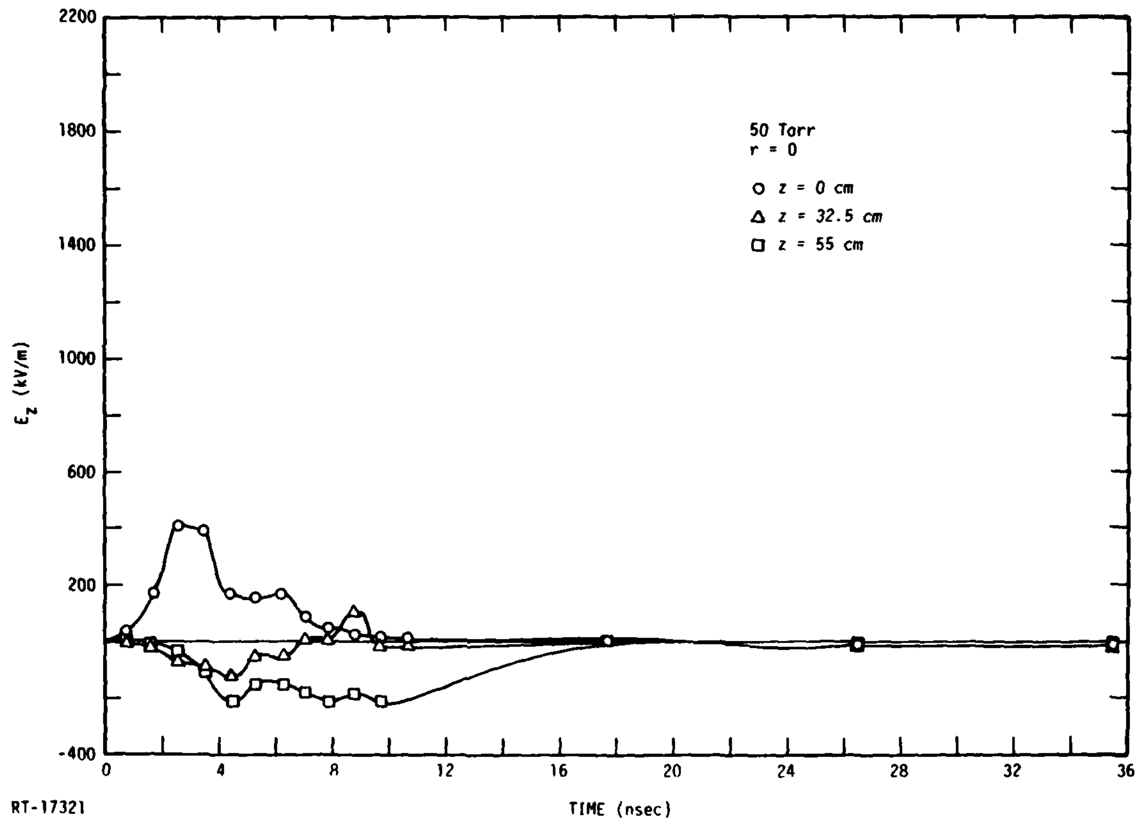

Figure 22. $E_z(t)$ at z = 0, 32.5, and 55 cm; r = 0 and a pressure of 50 torr.

REFERENCES

1. R. M. Gilbert, J. Klebers, A. Bromborsby, "Air Pressure Effects on Internal SGEMP: A Benchmark Experiment for Computer Code Validation," IEEE Transactions on Nuclear Science, NS-24, No. 6, December 1977.

2. R. E. Leadon, "Predicted Effect of Air Pressure on the IEMP Response of an Electron-Irradiated Cylinder," IRT Corporation Report 8168-001.

DISTRIBUTION LIST

DEPARTMENT OF DEFENSE

Assistant to the Secretary of Defense
Atomic Energy
ATTN: Executive Assistant

Defense Technical Information Center
12 cy ATTN: DD

Defense Intelligence Agency
ATTN: DB-4C

Defense Nuclear Agency
ATTN: DDST
2 cy ATTN: RAEV
4 cy ATTN: TITL

Field Command
Defense Nuclear Agency
ATTN: FCPR
ATTN: FCLMC

Field Command
Defense Nuclear Agency
Livermore Division
ATTN: FCPRL

Interservice Nuclear Weapons School
ATTN: TTV

Joint Chiefs of Staff
ATTN: J-3, WWMCCS Evaluation Office
ATTN: J-5, Nuclear Division

Joint Strat. Tgt. Planning Staff
ATTN: JLTW-2

National Communications System
ATTN: NCS-TS

Undersecretary of Defense for Rsch. & Engrg.
ATTN: Strategic & Space Systems (OS)

DEPARTMENT OF THE ARMY

BMD Advanced Technology Center
Department of the Army
ATTN: ATC-O

BMD Systems Command
Department of the Army
ATTN: BDMSC-H

Deputy Chief of Staff for Rsch. Dev. & Acq.
Department of the Army
ATTN: DAMA-CSS-N

Electronics Tech. & Devices Lab.
U.S. Army Electronics R&D Command
ATTN: DRSEL

U.S. Army Communications Sys. Agency
ATTN: CCM-AD-LB

DEPARTMENT OF THE ARMY (Continued)

Harry Diamond Laboratories
Department of the Army
ATTN: DELHD-N-RBC, R. Gilbert
ATTN: DELHD-I-TL
ATTN: DELHD-N-P

U.S. Army Foreign Science & Tech. Ctr.
ATTN: DRXST-IS-1

U.S. Army Missile R&D Command
ATTN: RSIC

DEPARTMENT OF THE NAVY

Naval Research Laboratory
ATTN: Code 6707, J. Davis
ATTN: Code 6701
ATTN: Code 6707, K. Whitney

Naval Surface Weapons Center
ATTN: Code F31

Strategic Systems Project Office
Department of the Navy
ATTN: NSP

DEPARTMENT OF THE AIR FORCE

Air Force Geophysics Laboratory
ATTN: PH, C. Pike

Air Force Weapons Laboratory, AFSC
ATTN: NXS
ATTN: NT
ATTN: SUL
2 cy ATTN: DYC

Deputy Chief of Staff
Research, Development, & Acq.
Department of the Air Force
ATTN: AFRDQSM

Rome Air Development Center
Air Force Systems Command
ATTN: ESR, E. Burke

Headquarters Space Division
Air Force Systems Command
ATTN: DYS

Headquarters Space Division
Air Force Systems Command
ATTN: SKF

Ballistic Missile Office
Air Force Systems Command
ATTN: MNNG
ATTN: MNNH

DEPARTMENT OF THE AIR FORCE (Continued)

Strategic Air Command
Department of the Air Force
ATTN: XPFS
ATTN: NRI-STINFO Library

OTHER GOVERNMENT AGENCY

NASA
Lewis Research Center
ATTN: Library
ATTN: C. Purvis
ATTN: N. Stevens

DEPARTMENT OF ENERGY CONTRACTORS

Lawrence Livermore Laboratory
ATTN: Document Control for Technical Information Dept. Library

Los Alamos Scientific Laboratory
ATTN: Document Control for MS 364

Sandia Laboratories
ATTN: Document Control for 3141

Sandia Laboratories
Livermore Laboratory
ATTN: Document Control for T. Dellin

DEPARTMENT OF DEFENSE CONTRACTORS

Aerospace Corp.
ATTN: V. Josephson
ATTN: J. Reinheimer
ATTN: Library

AVCO Research & Systems Group
ATTN: Library, A830

Boeing Co.
ATTN: P. Geren

Computer Sciences Corp.
ATTN: A. Schiff

Dikewood Industries, Inc.
ATTN: Technical Library

Dikewood Industries, Inc.
ATTN: K. Lee

EG&G Washington Analytical Services Center, Inc.
ATTN: Library

Eugene P. DePlomb
ATTN: E. DePlomb

Ford Aerospace & Communications Corp.
ATTN: A. Lewis
ATTN: Technical Library

General Electric Co.
ATTN: J. Peden

General Electric Company-TEMPO
ATTN: W. McNamara
ATTN: DASIAC

DEPARTMENT OF DEFENSE CONTRACTORS (Continued)

Hughes Aircraft Co.
ATTN: Technical Library

Hughes Aircraft Co.
ATTN: W. Scott
ATTN: E. Smith

Institute for Defense Analyses
ATTN: Classified Library

IRT Corp.
ATTN: Library
ATTN: D. Swift
ATTN: T. Buckman

JAYCOR
ATTN: Library
ATTN: E. Wenaas

JAYCOR
ATTN: R. Sullivan

Johns Hopkins University
ATTN: P. Partridge

Kaman Sciences Corp.
ATTN: W. Rich
ATTN: Library
ATTN: J. Lubell

Lockheed Missiles & Space Co., Inc.
ATTN: Dept. 85-85

McDonnell Douglas Corp.
ATTN: S. Schneider

Mission Research Corp.
ATTN: C. Longmire
ATTN: R. Stettnner

Mission Research Corp.-San Diego
ATTN: V. Van Lint
ATTN: Library

R&D Associates
ATTN: Technical Information Center
ATTN: C. MacDonald
ATTN: L. Schlessinger

Rockwell International Corp.
ATTN: Library

Science Applications, Inc.
ATTN: W. Chadsey

Spire Corp.
ATTN: R. Little

SRI International
ATTN: Library

Systems, Science & Software, Inc.
ATTN: A. Wilson
ATTN: Library

TRW Defense & Space Sys. Group
ATTN: E. Chivington
ATTN: Technical Information Center